Final report

1. Project details

Project title	Advanced Tips Enabled by Additive Manufacturing and Jointed Blades
File no.	64021-2062
Name of the funding scheme	EUDP
Project managing company / institution	Technical University of Denmark
CVR number (central business register)	DK30060946
Project partners	LM Wind Power
Submission date	26 February 2026

2. Summary

Project summary:

The purpose of the project

The purpose of the project was to develop novel wind turbine blade design solutions to increase performance of wind turbines, in particular advanced tip shapes enabled by emerging manufacturing methods such as additive manufacturing. Advanced blade design software had to be developed and validated, and novel aerofoils were tested in a wind tunnel.

Results, conclusions and perspective

- An advanced blade design software named AESOpt was developed capable of designing blades with curved tip shapes. The framework combined aerodynamic and structural analysis tools allowing for simultaneous design of aerodynamic and structural geometry of the blade. A key innovation was the implementation of an aerodynamic code (BEVC), which was capable of predicting the aerodynamic loading from curved tips at a numerical cost equivalent to standard aerodynamic codes used in industry. Additionally, a data-driven loads model was developed reducing the need for costly simulations in the design loop. To enable simultaneous design of aerofoils and blade shape, a data-driven model was developed based on a flow solver for predicting the performance of aerofoils. Together with BEVC this allowed for fast free-form design of wind turbine blades.
- Two conceptual blade designs were developed in the project, one blade optimized without an advanced tip, and another blade featuring a curved tip. The design study showed that 1-2% increase in

annual energy production could be achieved with blades featuring advanced blade tips without increasing loads or blade mass.
- Aerofoils dedicated to advanced blade tips were designed and wind tunnel tested by LM and a concept blade was designed using these aerofoils showing a 1.7% decrease in LCOE.

Projektresumé:

Formålet med projektet

Formålet med projektet var at udvikle nye løsninger til design af vindmøllevinger for at øge vindmøllers ydeevne, især avancerede vingeformer muliggjort af nye fremstillingsmetoder såsom additiv fremstilling. Avanceret vingedesignsoftware skulle udvikles og valideres, og nye vingeprofiler blev testet i en vindtunnel.

Resultater, konklusioner og perspektiv

- Der blev udviklet en avanceret vingedesignsoftware ved navn AESOpt, der er i stand til at designe vinger med krumme vingetipper. Frameworket kombinerede aerodynamiske og strukturelle analyseværktøjer, hvilket muliggjorde samtidig design af vingens aerodynamiske og strukturelle geometri. En vigtig innovation var implementeringen af en aerodynamisk kode (BEVC), som var i stand til at forudsige den aerodynamiske belastning fra krumme vingetipper med samme beregningstid som de aerodynamiske koder, der anvendes i industrien. Derudover blev der udviklet en datadrevet lastmodel, hvilket reducerede behovet for dyre simuleringer i designprocessen. For at muliggøre simultant design af vingeprofiler og vingeform, blev en datadrevet surrogatmodel for forudsigelse af aerodynamiske egenskaber af vingeprofiler. Sammen med BEVC tillod denne model effektiv og hurtig design af vingeform og profiler.
- Der blev udviklet to konceptuelle vingedesigns i projektet: en vinge optimeret uden en avanceret tip, og en anden vinge med en avanceret tip. Designstudiet viste, at der kunne opnås en stigning på 1-2% i den årlige energiproduktion med vinger med avancerede vingetipper.
- Vingeprofiler dedikeret til avancerede vingetipper blev designet og vindtunneltestet af LM og et konceptuelt vingedesign med brug af disse vingeprofiler, som viste en 1.7% reduktion af LCOE..

3. Project objectives

The objective of the project was to enable and demonstrate the potential for increased energy production of wind turbines by enabling larger rotors through the use of advanced aerodynamic and structural design methods. Specifically, the project explored the expanded design space made possible from modular or jointed blades combined with advanced manufacturing techniques such as additive manufacturing, which allow for advanced tip shapes incorporating large dihedral and sweep. Such advanced tips are known to have beneficial effects both aerodynamically to increase aerodynamic efficiency, but also to enable passive load alleviation.

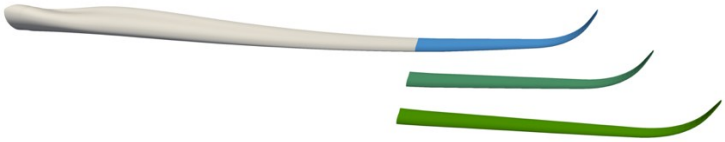

Figure 1: Imagined jointed blade with three interchangeable blade tips from the original application.

Jointed blade technology can enable larger rotor sizes for low wind areas, and therefore high value power production in markets with large wind energy utilization, since jointed blades are manufactured in two or more parts that can be assembled on-site overcoming critical transport constraints. Due to the high cost of the blade joint, so-called modular blades offer a more cost-effective alternative that allows for modularity in production and site-specific tailoring. Modular blades feature blade segments manufactured separately but assembled in a manufacturing plant and not on-site. While this technology does not tackle the transportation issues of large blades, it allows for a more cost-effective modular platform for sites where transportation is not a bottleneck.

To enable design of aerodynamically and structurally advanced blades, several challenges needed to be tackled in the design methods used for wind turbine blades. Traditional design tools based on Blade element momentum (BEM) methods do not account for out-of-plane tip geometries such as large pre-cone or sweep. Previous research at DTU had demonstrated that it was possible to model such geometries using medium-fidelity-modelling. The goal in the present project was to mature this modelling approach, both to increase its accuracy and to implement the model to also be suitable for gradient-based optimization. Secondly, methods to model advanced structural designs were needed, which required a flexible geometric parameterization and a fast and accurate structural models. The existing in-house 2D structural modelling tool, BECAS, and general purpose aeroelastic modelling tool HAWC2 were used for this purpose. Another goal of the project was to enable so-called freeform shape optimization in which not only the blade planform (chord, twist) was optimized but also the airfoils used on the blade were optimized. To achieve this in a time efficient manner the goal was to use a surrogate-based approach based on 2D CFD. Finally, to enable efficient aerostructural optimization of a wind turbine blade an optimization framework incorporating the above tools needed to be implemented, which should be capable of addressing a variety of optimization scenarios, ranging from pure structural optimization aerodynamic optimization and combined aerostructural optimization.

To explore the design potential possible through increased geometric complexity and advanced design methods, conceptual designs were developed and evaluated by LM Windpower, where a baseline design with a conventional blade shape and an advanced blade with a curved tip were developed by DTU.

The original objective of the project was to demonstrate advanced tip designs at full scale on a test turbine. However, for a variety of reasons the scope of the experimental demonstration was reduced to laboratory structural and wind tunnel aerodynamic tests. Specifically, canonical circular cylindrical shapes were manufactured and tested in DTU's Large Scale Facility with the intent to validate the combined 2D cross-sectional finite element and beam finite element models, and to aerodynamically verify airfoil designs developed within the project by LM.

4. Project implementation

The project was divided into two phases, Phase 1 with a 2-year duration and a Phase 2 with a 1-year duration, from the motivation that LM needed to be able to evaluate the potential of the developed technology and whether the planned full-scale experiment continued to be aligned with the overall business strategy. There was both risk involved in whether the developed blade technology would be sufficiently mature to test at full scale and whether the technology continued to be aligned with LM's overall technology roadmap, as well as risk involved in aligning the experiment with available test turbines owned by LM's mother company GE.

During first phase of the project the primary focus was to mature the design framework and underlying methods and models in WP1, as well as to carry out the laboratory scale structural experiments in WP3. The software

implementation progressed according to the project plan, resulting in a first version of the overall optimization framework that was delivered and installed on LM's HPC system as part of a two-day workshop.

During Phase 1 it became apparent that the full-scale field experiment would not be possible to carry out. Due to a variety of circumstances, it was agreed with the steering committee to apply to EUDP for a changed project scope without the full-scale experiment, and reduced budget for LM. During the 5 months period where the re-application was negotiated with EUDP, the project was paused.

In the final year of the project, conceptual designs were developed by DTU, that were evaluated in detail both by DTU and LM. LM designed an airfoil family, targetting balanced aerodynamic and aero-acoustic performance of blade tips, which were tested in the LM wind tunnel.

The project was concluded within the original time plan 31/12/2024.

5. Project results

The overall scope of the project was to enable design of advanced curved blade tips based on the hypothesis that advanced manufacturing and modular assembly techniques would result in an expanded design space, both aerodynamic and structural. The project achieved to deliver an optimization framework incorporating a highly advanced medium-fidelity aerodynamic model that combined with structural models provided the necessary foundation for exploring the advanced blade technologies. The project carried out a series of aerodynamic investigations into curved tip design, and two aerostructurally designed blades were made, one with optimized performance featuring a conventional tip shape, and another featuring an advanced curved tip. The following sections describes in detail what was achieved in the project.

WP1: Software implementation

The goal of Work Package 1 (WP1) was to develop a wind turbine blade design tool capable of modelling and optimizing blades featuring advanced structural designs and curved aeroelastically tailored blade tips. This entailed a ground-up development of a software that interfaced to a series of disciplines including geometric parameterization, structural modelling and aero-elastic modelling. Additionally, the tool should be able to model the blade at multiple fidelities including computational fluid dynamics (CFD). The resulting software was named AESOpt and in the following sub-sections a brief overview is given of the various sub-models in the framework.

Overall architecture

AESOpt is implemented in the Python programming language and uses the framework OpenMDAO as the backbone API for orchestrating the execution and coupling of different models. Figure 2 shows an Extended Design Structure Diagram (XDSM) of the full workflow of AESOpt, with sub-models highlighted in green along the diagram. Explicit variable connections are drawn between sub-components above the diagonal while implicit connections are drawn below the diagonal, which in the case of the present framework only involves the aero-elastic solver.

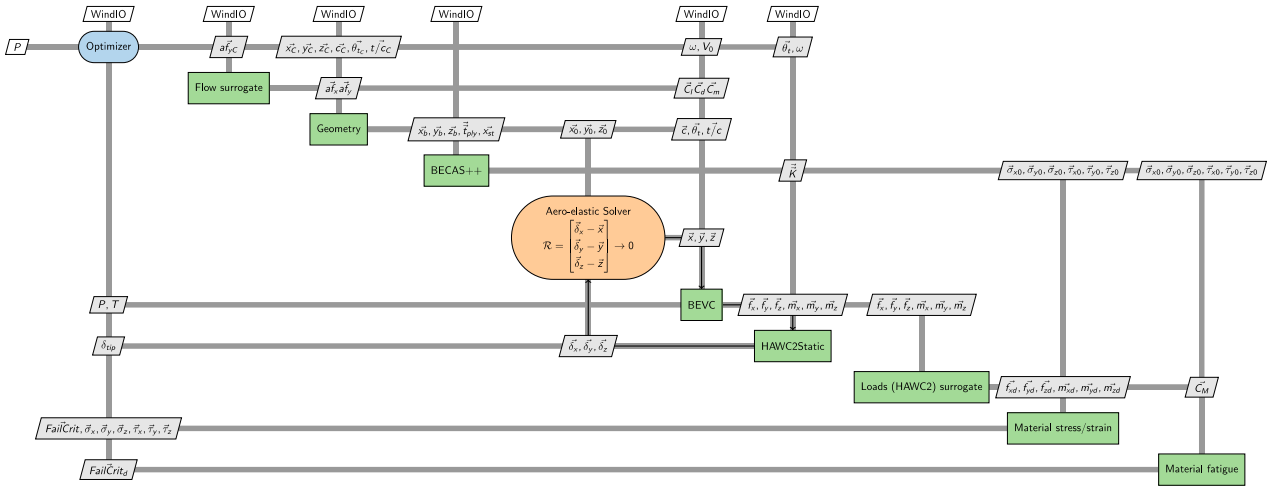

Figure 2: Extended Design Structure Diagram (XDSM) of the full workflow of AESOpt.

The choice of OpenMDAO as the backbone stems primarily from the ease with which analytical gradients can be computed across the framework, but also the modularity that results from implementing models using the OpenMDAO API.

Development practices, documentation and distribution

AESOpt is developed using git version control and hosted on a self-hosted GitLab instance provided by DTU. The framework consists of a main repository for the optimization framework, and individual repositories for the aerodynamic solver BEVC, the cross-sectional mesher CSMesher, and declares dependencies on other packages, such as the structural solver BECAS++ and HAWC2. An integral part of the development practices is to write unit tests for all committed code, and test the code using GitLab's continuous integration (CI) platform. Since AESOpt is written in Python, the code is distributed as a Python wheel and available via an access-restricted package registry, which makes installation relatively easy although AESOpt has a series of external dependencies that require license files to be installed. AESOpt is documented using Jupyter Book and hosted with GitLab Pages, see an example in Figure 3. The documentation includes installation instructions, API docs for all classes in the codebase as well as a series of tutorials describing common use cases of the framework.

Figure 3: AESOpt documentation example.

Wind Turbine Parameterization

WindIO[1] is used as the primary input specification for defining a wind turbine. The idea behind windIO is to have a community defined ontology for describing a wind energy system that is not tool-specific, allowing more easily to communicate a wind turbine design with collaborators. Besides using windIO to describe the wind turbine, AESOpt requires modelling specific inputs that is specified separately.

To enable easier conversion of inputs between different modelling tools, a stand-alone software package WindIO Converter was developed, which handles the conversion of windIO to AESOptIO and windIO to HAWC2, and vice versa. The package also facilitates easier inspection and auto-documentation of variables and data structures.

Geometric and Structural Parameterization

AESOpt implements the geometric and structural parameterization of windIO and enables the user to define spline-based design variables to smoothly vary quantities like blade chord and twist, as well as internal structural laminate thicknesses and placement of these. The structural parameterization allows to define composite layers with individual spanwise extent, as well as arbitrary changes to the blade topology along the span. This

[1] https://github.com/IEAWindSystems/windIO, https://doi.org/10.5281/zenodo.15191296

for example allows to model blades where the tip features a composite structure tailored towards a high-curvature aerodynamic shape. To enable efficient gradient-based optimization, gradients of the structural geometry with respect to user-defined design variables are computed through a mix of analytical and algorithmic differentiation.

Cross-sectional Structural Modelling

To model the internal composite structure of a wind turbine blade, AESOpt interfaces to BECAS. BECAS generates the fully populated stiffness and inertia matrices based on a 2D finite element mesh representing the actual geometry of the cross-section. The computed properties can subsequently be used in a beam finite element code, for example HAWC2. Cross-sectional meshes are generated using a simple meshing tool developed within the present project called CSMesher, which is written in a combination of Fortran and Python. The tool is algorithmically differentiated using Tapenade to produce machine accurate gradients supporting both forward and reverse (adjoint) mode gradient propagation. An example of a cross-sectional mesh can be seen in Figure 4. As is evident, the cross-sectional mesher does not model all details seen in actual manufactured blades, but for conceptual design this level of detail was judged as sufficient. Work is on-going in other projects to develop a cross-sectional mesher with significantly higher geometric detail, but this mesher was not available during the present project.

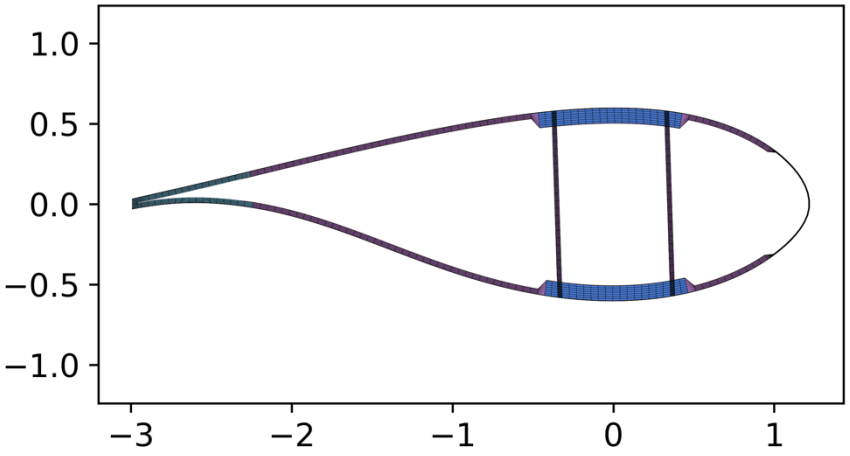

Figure 4: Example cross-sectional mesh

Strains were evaluated in the cross-section based on multiplication of unit-strains computed with BECAS and design load vectors and aggregated using the Kreisselmeier-Steinhauser Function to a single value for each cross-section.

Aerodynamic modelling: BEVC

The aerodynamic module developed and used in the project is the blade element vortex cylinder (BEVC), which is a multi-fidelity engineering aerodynamic modeling tool. The advantages of this modeling complex compared to conventional blade element momentum (BEM) method is its ability to model the effects of curved blade geometry and non-planar rotor on the wake and consequently on the loads and inductions. The BEM method is a combination of the blade element theory (BET) and the momentum theory (MT) and has been the main working horse for in aerodynamic and aeroelastic calculations of modern wind turbines. Despite its widely

spread use, it has various assumptions inherited from the momentum theory, which hinders the application of the modeling of curved blades and non-planar rotors. Despite the BET is able to correctly model the projections between the 3-D flow and the 2-D airfoil using the cross-flow principle, the MT implicitly assumes the blades are straight and form a planar rotor. To solve this issue, the influence of blade sweep and prebend on the wake geometry and hence on the inductions should be correctly modeled.

Firstly, the influence of blade prebend on the wake geometry is summarized. For a non-planar rotor, the surface swept by the blade will be non-planar and the trailed wake will emanate from it. Compared to a planar rotor, the starting positions of the trailed vortex will begin further upstream or downstream compared to it. This will result in a difference in the axial induction. Furthermore, according to the Kutta-Joukowski analysis, which is equivalent to the projection of the lift force, it is discovered that the radial induction is important to be modeled for non-planar rotors. To model these two effects, the vortex cylinder (VC) model is used, replacing the MT. The starting position of the vortex cylinders follow the actual surface swept by the blades and the influence on the axial and radial inductions are then modeled. When the rotor is planar and neglecting the wake rotation effect, which is negligible for ordinary wind turbines at the optimal operating conditions, the results will then tend to BEM results. Then, the rotor's non-planar effects are modeled with the blade element vortex cylinder (BEVC) model, which is the coupling of BET and VC.

Secondly, the influence of blade sweep on the wake geometry is summarized. For a swept blade, there are two major effects on the wake geometry should be modeled. First, the curved bound vortex follows the 1/4 chord line (lifting-line) of the blade and is then swept. Then, there will be influence due to the curved bound vortex on itself. Second, since the trailed vortices start to trail from the 1/4 chord line of the blade, the starting position will then be shifted compared to that of a straight blade. For example, for a backward swept blade, the starting position of the trailed vortex will then be later compared to a straight blade. In a previous study, it has been shown that both effects should be included to correctly model the blade sweep effects. Otherwise, if only the trailed vortex influence is included while the curved bound vortex influence is neglected, the gain due to the blade's backward sweep will be overestimated. For the curved bound vortex influence, it is simply modeled using the Biot-Savart law, with the calculation point placed at the 3/4 chord point and calculated with the 3-D effect minus the local 2-D effect. For the trailed vortex effect, a simplified lifting-line method is implemented. It is a coupled near- and far-wake model, where the near wake is defined as the first quarter revolution of the trailed wake of the own blade and is modeled using indicial functions with empirical equations. For the far wake, two different fidelities (NW-MT-VC and NW-VC) are possible, either from a simple scaling of the momentum theory or from a far wake vortex cylinder model. For NW-MT-VC, the far wake induction is from the scaled momentum theory but the radial induction is calculated from the vortex cylinder model. For the later, the starting position of the far wake is further downstream of the rotor disc. The near and far wake models are coupled together to get the total inductions, which is having similar thrust level as a BEM method with Prandtl's tip-loss correction. Similarly, the radial induction is from the full trailed wake vortex cylinder.

Thirdly, the influence of blade sweep and prebend combined is investigated. Investigations are performed using the CFD results and using conclusions derived from the BEM method. It is discovered that for ordinary operational conditions, including both optimal operational conditions and lower loading conditions, the blade sweep and prebend effects can be well approximated by superpositioning of the pure swept blade and the pure prebent blade. As a result, when modeling a general combined curved blade, it is possible to combine the non-planar effects from the VC model and the sweep effects from the curved bound vortex and the near wake model. Then, the results from the coupled NW-MT-VC and NW-VC models are expected to well approximate the results.

Numerical investigations are performed on different curved blades, including swept blades, prebent blades and blades with both sweep and prebend combined. For abbreviations, only one blade with both backward sweep and upwind prebend combined at the optimal operational condition is used for comparison here. The blade is modified based on the IEA 10MW RWT and has a radius of 99 m, including a hub radius of 2.8 m.

The operational condition is with a free wind speed of 8 m/s and a tip speed ratio of 10.58. The thrust coefficient predicted by the BEM method is 0.90. The low- and mid-fidelity engineering aerodynamic models used for the comparison includes BEM, BEVC, NW-MT-VC and NW-VC. Further, two higher-fidelity aerodynamic models, including a free wake lifting line (LL) model in the MIRAS code and a RANS CFD solver in the EllipSys3D. To better show the influence of the curved blade geometry on the loads, the difference in loads of the curved blade compared to the baseline straight blade is used for the comparison.

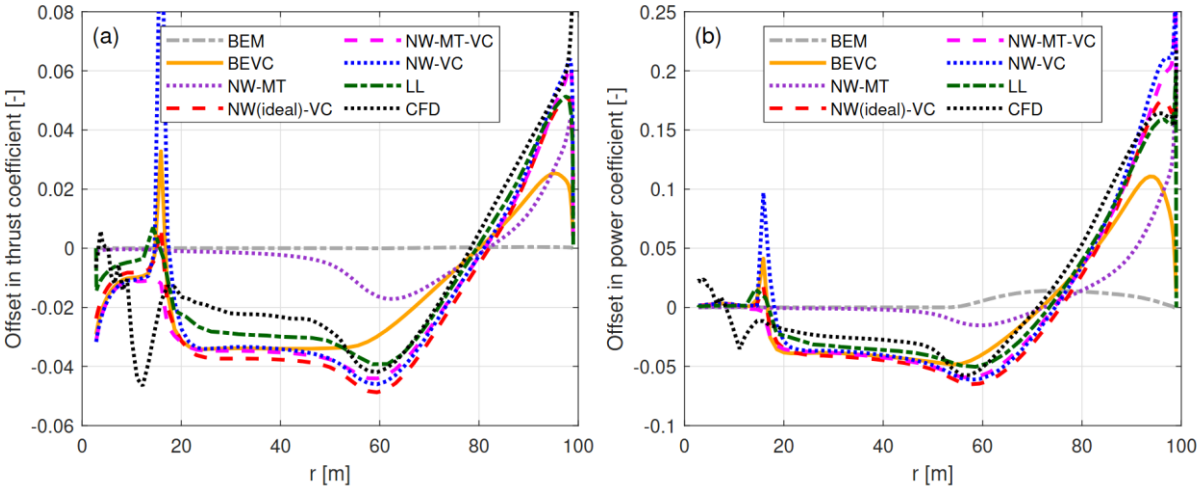

Figure 5: The difference in thrust coefficient (a) and simplified power coefficient (b) of the curved blade with both backward sweep and upwind prebend combined compared to the baseline straight blade.

For the curved blade, both LL and CFD results show a load redistribution pattern, which is also documented in previous works. Compared to the baseline straight blade, loads are lower from the blade root to a radius of 80 m and higher from 80 m to the blade tip. The BEM method predicts nearly the same loads for the curved blades as the baseline straight blade, which is expected since it does not account for prebend or sweep effects. The BEVC method capture the load redistribution patterns but underestimate their magnitudes, as it model only prebend effects. The coupled models NW-VC and NW-MT-VC show good agreement with LL and CFD, with small discrepancies near the blade tip (radius larger than 90 m).

The BEVC code is firstly coded using FORTRAN and then the algorithmic differentiation (AD) method is applied to the code, so that the gradients of both forward mode and backward mode are obtained. The results and gradients are linked into a python interface using C-types binding. As a result, the BEVC code is suitable to be used in the AESOpt framework for gradient-based aeroelastic optimization tasks.

Extensions of HAWC2 for gradient-based optimization

Historically, HAWC2 has been developed as an executable, which takes as input several text files and outputs time series. In (J. C. Heinz et al., Fluid–structure interaction computations for geometrically resolved rotor simulations using CFD) HAWC2 was compiled as a library and coupled to the CFD solver EllipSys3D using OpenMDAO. At each time step, HAWC2 would receive aerodynamic loads and provide the new blade displacement and rotation. The FSI coupling was further improved in (S. G. Horcas et al., Vibrations of wind turbine blades in standstill: Mapping the influence of the inflow angles), which replaced OpenMDAO in favor of a custom Python package. It is from this work that we have started.

While previous FSI couplings focused on time simulations, for the present work we needed a static solution. This led to the development of a new static solver for HAWC2. The static solver uses a sparse Newton method

to compute the equilibrium configuration for the assigned aerodynamic loading. The HAWC2 static solver algorithm has been extended to floating wind turbines in (R. Riva et al., Incorporation of floater rotation and displacement in a static wind farm simulator), and to controlled systems in (A. M. Antunes et al., Static Response of Beam-Like Structures for the Analysis of Wind Turbine Blades With Different Levels of Fidelity).

Our previous in-house blade design tool HAWTOpt2 relied on HAWCStab2, and therefore required writing and reading text files, which complicated parallel processing. For AESOpt we wanted to avoid this problem, and therefore read and write data in memory. The newly developed workflow allows to have several HAWC2 instances running in parallel, and update several inputs, for example the blade structural data and rotor speed, through python functions.

HAWC2 has also been extended to provide the gradient of the blade displacement, rotation and loads with respect to the structural parameters. The analytical gradient of the equation of motion has been computed, which naturally requires the gradient of each component. The components gradient is obtained by using a combination of the complex step method with analytical diffentiation of the static solver. This was achieved by a tool that automatically complexifies the HAWC2 source code. At the time of writing, some gradients verify well against finite differences, while others require further debugging. Currently the gradient computation is only available in a forward matrix free mode. In future work reverse (adjoint) mode will be implemented to enable solving large scale optimization problems.

During the last part of the project, we have started to port the features developed during AMTip to HAWC2lib, a publicly available python package that allows using HAWC2 as a library.

Aero-elastic Analysis

The nonlinear aeroelastic coupling between BEVC and the static multibody solver in HAWC2 is solved using OpenMDAO's Block Gauss-Seidel fixed-point solver. The solver applies Aitkin under-relaxation of the states to accelerate and stabilize convergence of the problem. In an optimization context, robust convergence of the aeroelastic coupling is essential to ensure accurate responses and gradients of these. OpenMDAO facilitates computation of gradients of the coupled solution, and while the project had the ambition to achieve this capability, algorithmically differentiated gradients were only available in the aerodynamic solver, while finite-differenced gradients were computed for the beam solver.

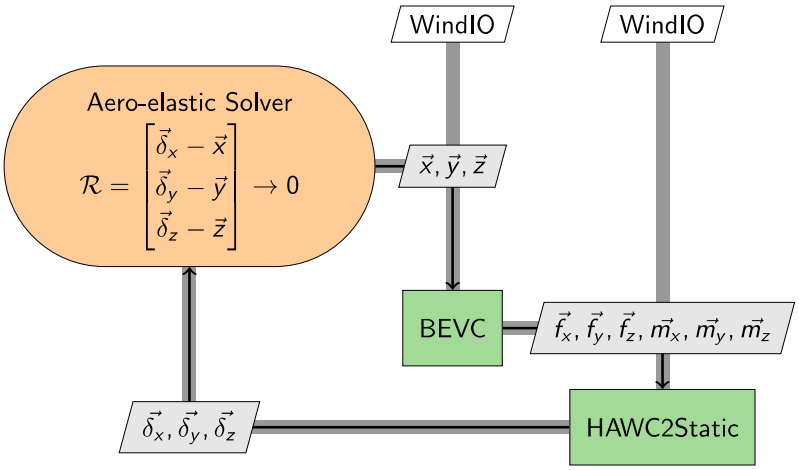

Figure 6: Static aeroelastic solution process coupling BEVC and the static solver in HAWC2.

Loads surrogate

A machine learning model is trained on time-domain aeroelastic load simulations in order to provide a load surrogate model from static rotor loads input to lifetime wind turbine design loads, and evaluated on the IEA-3.4-130-RWT with a range of design variations, as described in detail in Barlas et al.[2]. The IEA-3.4-130-RWT is simulated in HAWC2 in representative IEC-type of design load cases for ultimate (DLC 1.3) and fatigue (DLC 1.2) loads, resulting in total of 756 10-min load cases. In all cases, 18 turbulent seeds per wind speed bin from cut-in to cut-out with 3 yaw misalignment angles (±8deg) are used, and fatigue loads are calculated with m=4 (m=10 for blades), Neq = 1e7, Vref = 37.5 m/s, and k =2. Parametric design variations around the baseline rotor design are also defined consisting of scaling the blade, tip-speed ratio (TSR) variations, and pitch ramp settings variations in below rated operation. Each input variable follows a uniform distribution and is independent from the others. The joint distribution is sampled using a quasi-random Halton sequence with scrambling, using the OpenTURNS implementation. The Halton sequence allows to evenly cover the input domain, while the scrambling reduces the correlation between the inputs. A total of 100 design cases are simulated where, apart from the baseline IEA-3.4-130-RWT, the blades are stretched [0% to +10%], the TSR is varied [-10% to +10%], and the pitch ramp settings in below rated operation are varied [-3deg to +3deg]. This results in a realistic variation of blade designs for the given wind turbine platform. The design space with the input samples is shown in Figure 7, while the range of representative blade distributed parameters and minimum pitch settings are shown in Figure 8 and Figure 9. From all cases, 79% are used for training, 20% for validation and 1% for testing. The input to the surrogate model comprises the scaling factors for blade length, TSR and pitch and the pre-calculated steady state loads (internal forces and moments on all blade nodes) and the output comprises the blade ultimate and lifetime fatigue loads (internal forces and moments on all blade nodes) and turbine ultimate and fatigue loads (internal moments on main components). The calculated output loads comprise the absolute maximum from all simulated load cases. The input steady-state (ss) reaction forces (F) and moments (M) across x, y and z directions distribution along the blade span (Z) for all simulated cases is shown in Figure 10, with the calculated blade ultimate reaction forces and moments distribution in Figure 11, the calculated blade fatigue reaction forces and moments distribution in Figure 12, and the calculated turbine component ultimate and fatigue loads in Figure 13.

[2] Barlas, T., Göçmen, T., & Riva, R. (2024). Development of a machine learning model for wind turbine fatigue and ultimate loads based on static loads. In *The Science of Making Torque from Wind (TORQUE 2024):* Article 052009 IOP Publishing. https://doi.org/10.1088/1742-6596/2767/5/052009

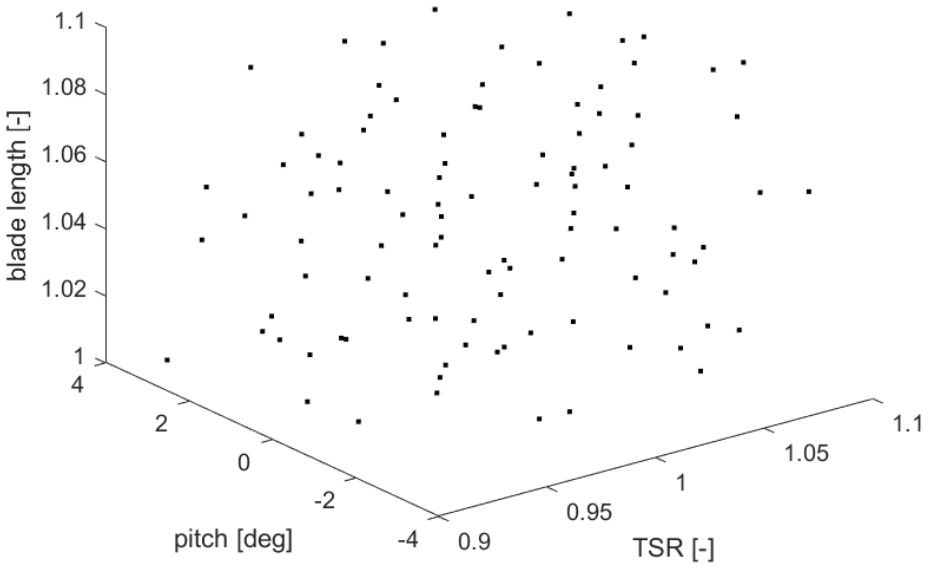

Figure 7: Design space and input samples.

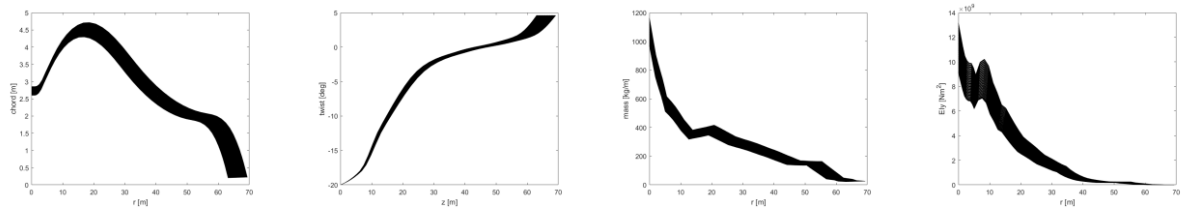

Chord. *Twist.* *Mass.* *Flapwise stiffness.*

Figure 8: Spanwise distribution of design parameters for training samples.

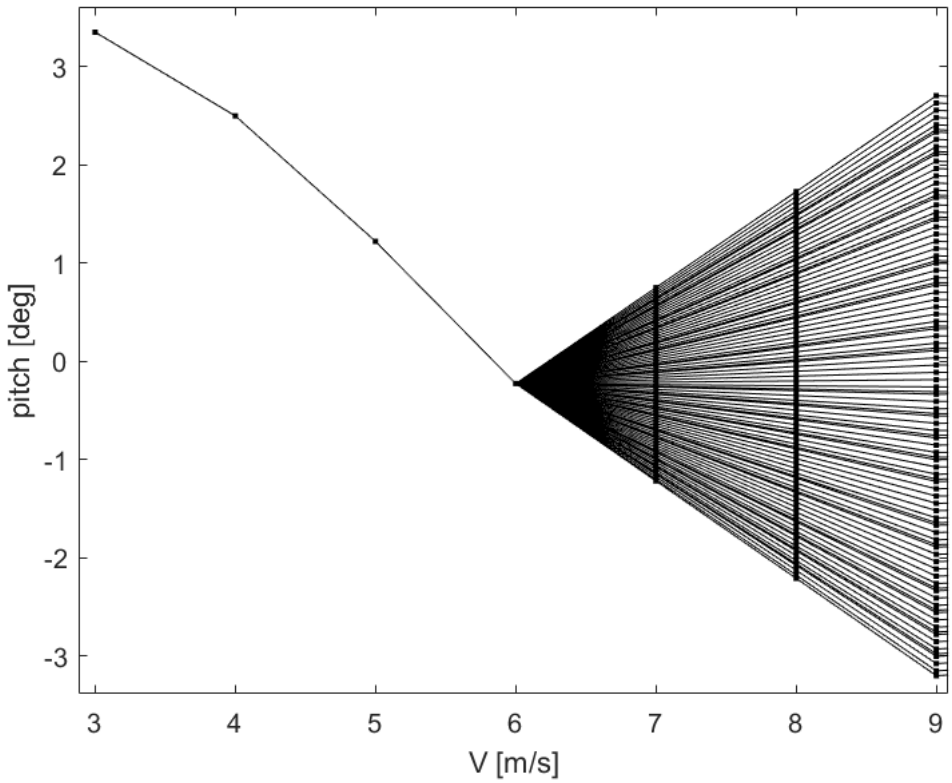

Figure 9: Range of input data for minimum pitch in below rated operation.

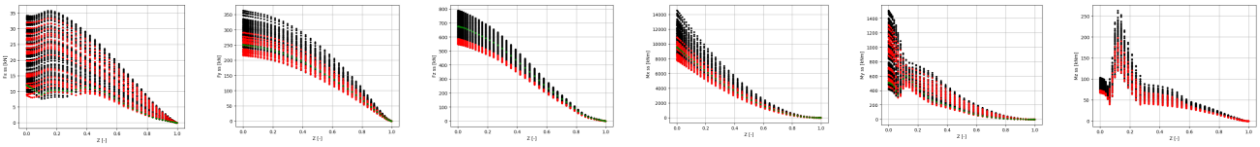

Figure 10: Steady-state internal forces and moments along the normalized blade span (Z) for all simulated cases (black: training set, red: validation set, green: test set).

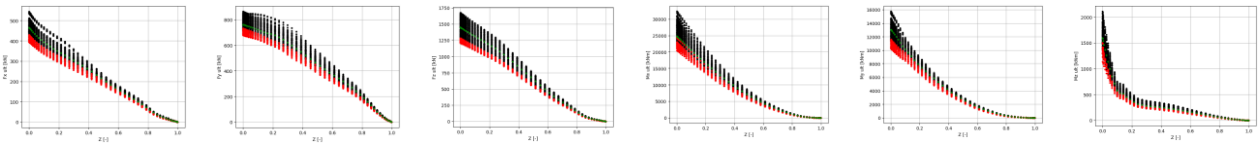

Figure 11: Ultimate internal forces and moments along the normalized blade span (Z) for all simulated cases (black: training set, red: validation set, green: test set).

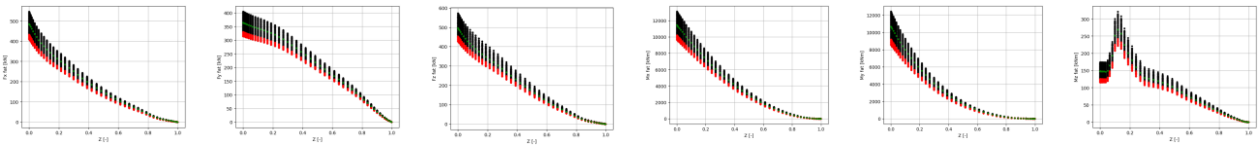

Figure 12: Fatigue internal forces and moments along the normalized blade span (Z) for all simulated cases (black: training set, red: validation set, green: test set).

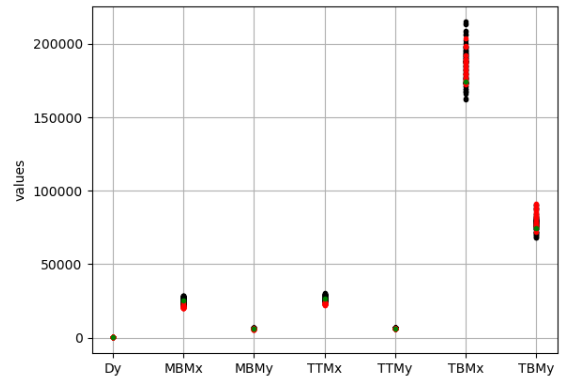

Ultimate.

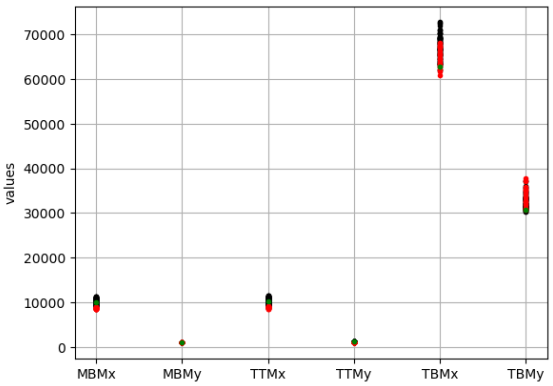

Fatigue.

Figure 13: Ultimate and fatigue wind turbine component loads for all simulated cases (Dy: flapwise tip deflection [m], MBMx: main bearing tilt moment [kNm], MBMy: main bearing yaw moment [kNm], TTMx: tower top fore-aft moment [kNm], TTMy: tower top side-side moment.

The surrogate model utilizes feed-forward neural networks as the basis using TensorFlow with the Keras API and 3 layers. The model parameters are tuned using the Keras tuner grid search, for a range of objective metrics, initialization functions, activation functions and number of neurons per layer. The hyperparameter space explored in the grid search consists of a range of objective metrics (mean square error, mean absolute percentage error, mean absolute error), initialization functions (glorot uniform, random uniform), activation functions (tanh, sigmoid, ReLU) and number of neurons per layer (100-500 with a step of 10). Prior to training, the input and output datasets are processed with a standard scaler, fitted on the training set. Four different models are trained for blade ultimate loads, blade fatigue loads, turbine ultimate loads, and turbine fatigue loads, resulting in the best models (minimizing prediction error).

The comparison of the surrogate model predictions with the time-domain simulation results for the blade ultimate internal forces and moments distribution is shown in Figure 14, and for the blade fatigue internal forces and moments distribution is shown in Figure 15. The comparison of the surrogate model predictions with the time-domain simulation results for the turbine component ultimate and fatigue loads is shown in Figure 16. The comparison is on average accurate (mean error 0.5-2.2%, max error 1,4-2.4%), with only some deviations of ultimate loads close to the root (max error 11.7%). Apart from the max error on the blade root and tower base ultimate loads, the rest of the average and max error are well within the expected uncertainty of aeroelastic models and load validation.

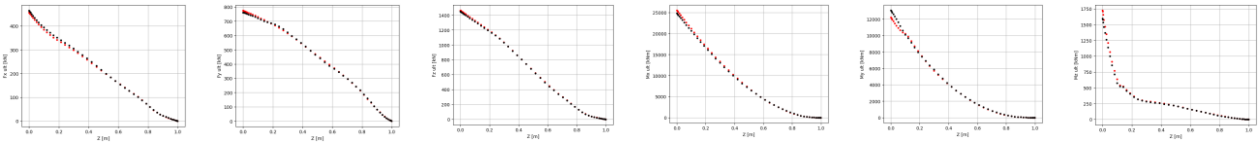

Figure 14: Ultimate internal forces and moments along the normalized blade span (Z) for all simulated cases (black: training set, red: validation set, green: test set).

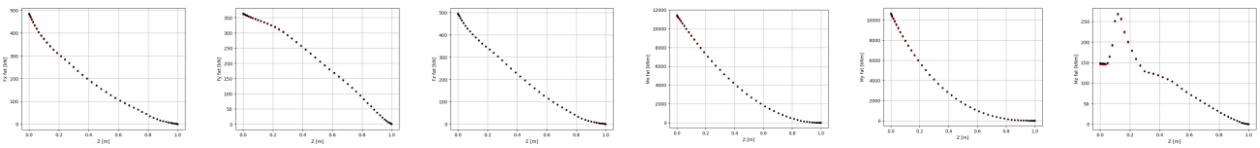

Figure 15: Fatigue internal forces and moments along the normalized blade span (Z) for all simulated cases (black: training set, red: validation set, green: test set).

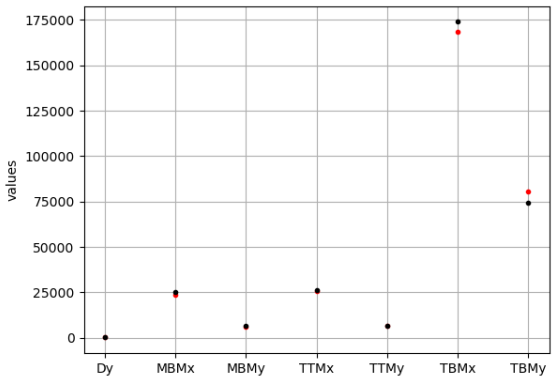

Ultimate.

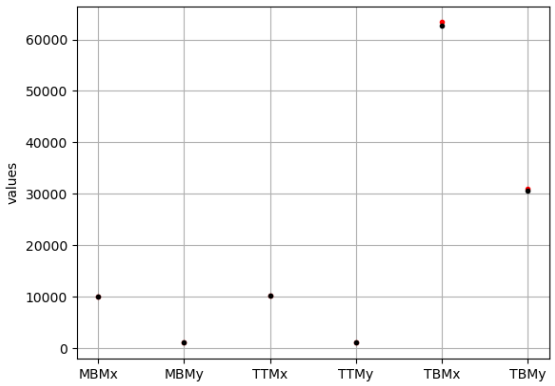

Fatigue.

Figure 16: Ultimate and fatigue wind turbine component loads for all simulated cases (Dy: flapwise tip deflection [m], MBMx: main bearing tilt moment [kNm], MBMy: main bearing yaw moment [kNm], TTMx: tower top fore-aft moment [kNm], TTMy: tower top side-side moment [kNm].

The ultimate and lifetime fatigue load predictions of the surrogate model provide good accuracy for design variations within the design space training set. Utilizing only steady-state blade load input data can provide fast design loads evaluation for design optimization. In this work, apart from TSR and pitch variations in below-rated operation, only normal blade scaling has been utilized as input. In future work, it will be important to explore other relevant variations of blade design scaling options with respect to the planform and structural properties. Finally, since the current surrogate model is applicable only for the design conditions of the baseline wind turbine, site-dependent design input parameters could also be considered, so that the model could be utilized in multi-point design optimization studies.

The load surrogate model has been coupled to AESOpt via a newly developed python package named surrogates_interface. This package aims to:

- Provide a common interface to several surrogate model libraries. During AMTip we have added support for TensorFlow and SMT, and recently also for PyTorch.
- Provide several transformations for the input and output data (standard scaler, min-max scaler and so on), which match the ones available in scikit-learn, and add the analytical gradient.
- Cover the entire surrogate model evaluation process: direct input transformation, evaluation of the surrogate and inverse output transformation.
- Provide the analytical gradient.
- Save the entire surrogate model, including input and output transformations, in a portable format.
- Couple the surrogate with OpenMDAO.

The surrogates_interface package has been described in (R. Riva et al., Incorporation of floater rotation and displacement in a static wind farm simulator).

The coupling of the surrogate model with AESOpt is complemented by gradient-friendly versions of the absolute value and max functions, which are also analytically linearized.

Freeform Shape Optimization using a Flow Surrogate

Freeform shape optimization of wind turbine blades refers to the simultaneous design of both the overall blade shape (planform with chord, twist and relative thickness), and the cross-sectional airfoil shapes along the blade. A medium-fidelity aerodynamics code normally uses pre-computed airfoil data based on a given set of airfoils, but when allowing the airfoil shapes to change, airfoil data will change along with the airfoil shape requiring re-computation using a tool like Xfoil or 2D CFD. To enable freeform shape optimization in a medium-

fidelity framework the aim was to develop a faster approach than direct computation of airfoil flows using a surrogate-based approach in which the 2D CFD solver EllipSys2D was evaluated across a wide range of shapes, which would then be used to train a surrogate model appropriate for airfoil optimization. Two approaches were pursued: One using a Gaussian process model Kriging and another one using a machine learning-based model. Both approaches relied on the same parameterization of the airfoil using the so-called Class Shape Transformation (CST) parameterization.

2D CFD-based training data

The FlowOpt2D framework was used to run the design of experiments that sampled a wide range of shapes, to make a suitable database for training the surrogates. FlowOpt2D interfaces to the EllipSys2D CFD solver and mesh generator HypGrid2D through PyEllipSys that defines common interfaces to all the EllipSys tools. All computations were performed assuming steady-state flow on a computational mesh with 256x128 cells. Two databases were made, one assuming fully turbulent boundary layer flow with the K-omega SST turbulence model, and another including modelling of laminar-to-turbulent transition using the Drela-Giles transition model. Figure 17 shows an example of the sampled airfoil shapes and corresponding lift to drag ratios vs lift coefficient.

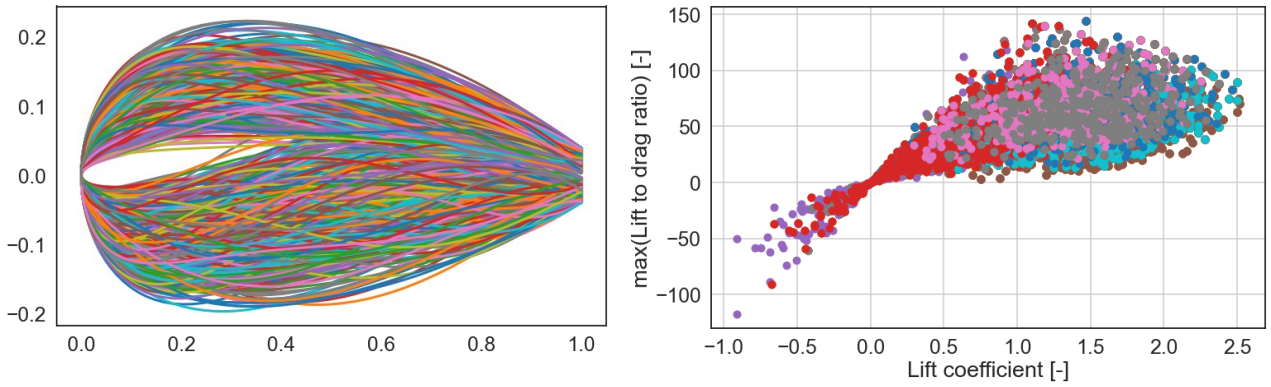

Figure 17: Sampled shapes and corresponding lift to drag ratios.

Kriging-based surrogate model

The openly available SMT package was used as basis for the Kriging-based surrogate approach combined with a light-weight wrapper in OpenMDAO. As a preliminary test, a simple optimization was set up to test the capabilities of the surrogate-based approach. Figure 18 shows an example of a gradient-based optimization of a single airfoil optimized to maximize lift-to-drag ratios with a balance between turbulent flow performance and free transition.

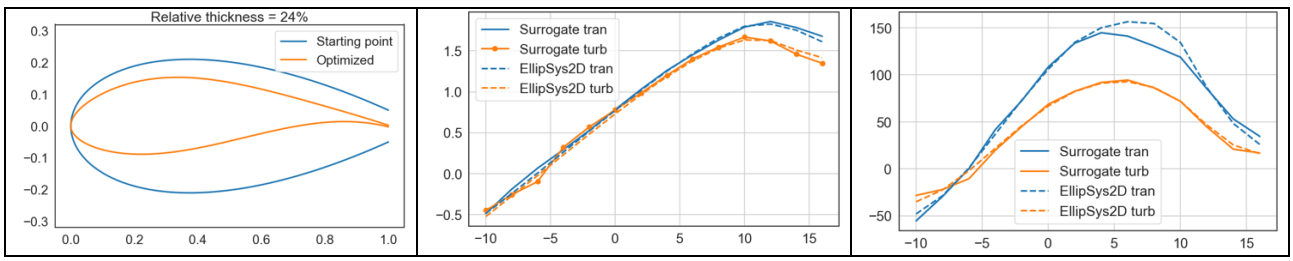

Figure 18: Example optimization of an airfoil compared to EllipSys2D evaluations of the optimized shape.

In AESOpt a workflow was developed around the SMT-based surrogate allowing to optimize an arbitrary number of airfoils along the span of the blade. Similar to the single airfoil optimization, constraints on geometric

properties such as relative thickness, as well as aerodynamic characteristics such as maximum lift coefficient could be constrained. The resulting workflow outputs C_l, Cd, C_m polars which could dynamically be connected to the BEVC aerodynamic solver. Figure 19 shows a workflow diagram of the aerodynamics-only freeform optimization setup. Including optimization of the airfoil shapes along the blade increases the number of design variables significantly, and to enable fast and numerically stable optimization it was key that the flow surrogate and the aerodynamic solver BEVC supported computation of analytical gradients, allowing us to solve an adjoint problem where the computational cost of the optimization becomes invariant to the number of design variables.

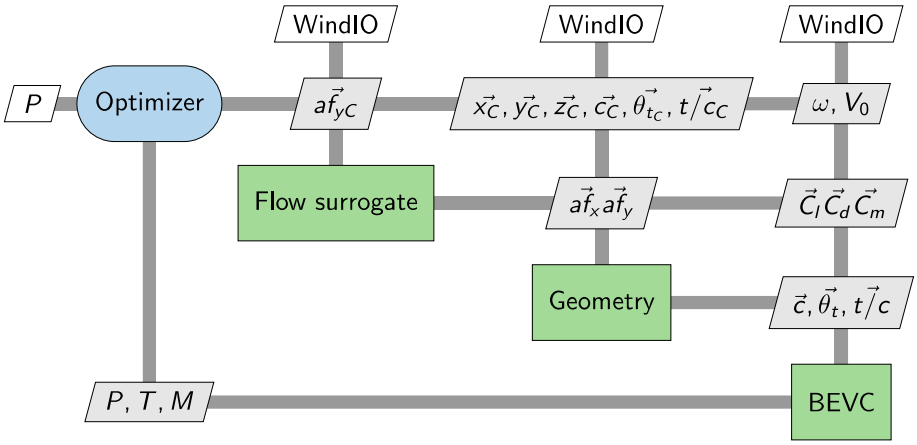

Figure 19: Aerodynamic freeform optimization workflow in AESOpt.

High-fidelity aeroelastic analysis using 3D CFD

Aeroelastic analysis using high-fidelity Computational Fluid Dynamics (CFD) was implemented in AESOpt enabling direct comparison between an aeroelastic solution based on BEVC with that using 3D CFD. This work was partially funded by other projects and a large offshore blade was therefore used to carry out the multi-fidelity validation between BEVC and the EllipSys3D CFD solver coupled to HAWC2. Figure 21 shows the 3D steady-state flowfield computed for the IEA 22 MW RWT at 10 m/s. See Zahle et al for more details on this validation.[3]

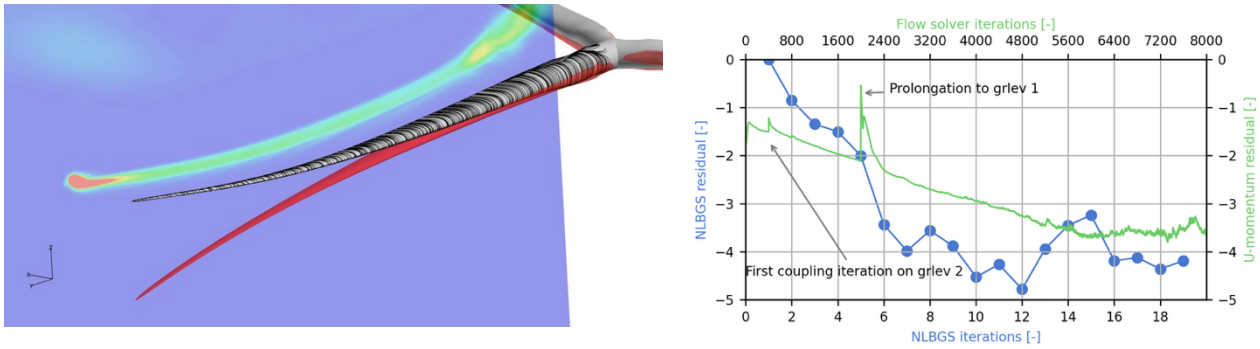

Figure 20: Left, visualisation of the flowfield around the deflected blade computed at 8 m/s. Right, the convergence history of the coupled steady-state FSI solver implemented in AESOpt.

[3] Zahle, F., Li, A., Lønbæk, K., Sørensen, N. N., & Riva, R. (2024). Multi-fidelity, steady-state aeroelastic modelling of a 22-megawatt wind turbine. In *The Science of Making Torque from Wind (TORQUE 2024):* Article 022065 IOP Publishing. https://doi.org/10.1088/1742-6596/2767/2/022065

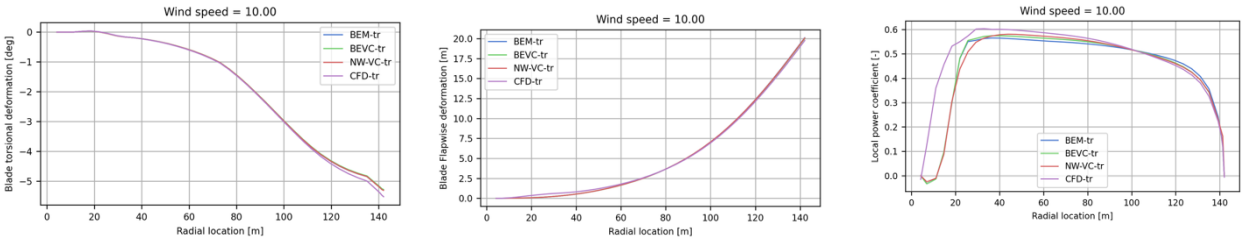

Figure 21: Aeroelastic state-state computed at 10 m/s, showing left blade torsion, middle, flapwise defiection, and right local power coefficient.

WP2: Concept development

In this work package the design tools developed in WP1 were applied to a range of different conceptual design studies. Firstly, AESOpt was used to carry out a freeform aerodynamic design of a blade where six cross-sections along the blade as well as the blade chord and twist were optimized using the developed 2D flow surrogate. Secondly, AESOpt was used to aerostructurally optimize the blade AMTB1 which had a conventional blade tip, but otherwise optimized fully. Following this, the design space for curved blade tips was explored with a variety of optimization problems with varying constraints. The three chosen designs from this study were validated with 3D CFD. Finally the AMTB2 blade which featured a curved blade tip was optimized using the learnings from the previous study. In the following sections details of these studies are presented.

Freeform aerodynamic design of blades

To demonstrate the freeform optimization capabilities implemented in AESOpt, an aerodynamic rotor optimization was carried out. A modified version of the IEA 3.4 MW RWT used as baseline, and the optimization problem solved is summarized below. The problem was solved using the reverse propagation capabilities of BEVC combined with the analytical surrogate and could therefore be executed on a desktop computer.

- Objective: max(AEP) based on mixed polars (30% turbulent, 70% free transition)
- Design variables (82 total):
  - 6 airfoil sections at *r/R*=[0.2, 0.4, 0.6, 0.8, 0.9, 1.0] each with 9 design variables
  - Chord, twist
  - Pitch, tsr
- Constraints:
  - Blade absolute thickness,
  - Rated torque, thrust, flapwise moment
  - Airfoil geometric compatibility

Figure 22 shows the resulting airfoil shapes along the blade, and the optimized planform. The performance of the freeform optimized blade is marginally improved compared to the baseline IEA 3.4 MW RWT, which matches the expectations. In fact, combined planform and airfoil optimization was not expected in itself to outperform a process where firstly airfoils were optimized individually, followed by an aerodynamic design. The major benefit of a freeform approach is, however, expected when also including the structural and aeroelastic design in the optimization problem, since the airfoil geometry can be customized exactly to the structural design and desired aeroelastic response. This, however, lied beyond the scope of the present project and remains to be demonstrated in future work. Figure 23 shows the clean (green) and rough (blue) polars (lift coefficient vs angle of attack) as well as lift-to-drag coefficient vs angle of attack, comparing in solid lines the surrogate predictions with 2D CFD evaluations of the airfoils. Overall a quite good agreement was found between the Kriging-based surrogate and CFD evaluations, but we expect to be able to improve the accuracy of the model

using neural-net based models. Work was initiated in the project on such a model, but was not finalized, and remains to be completed in a future project.

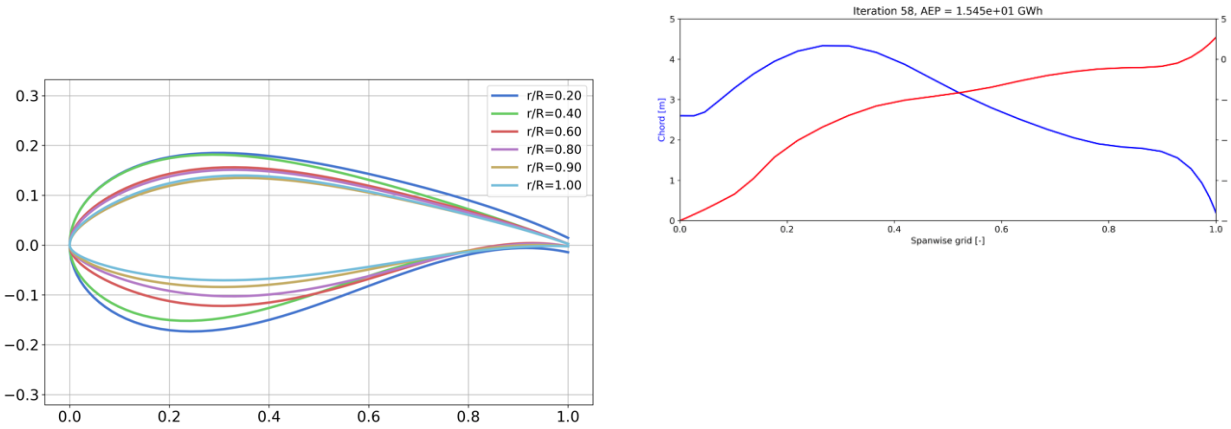

Figure 22: Optimized airfoil shapes and blade planform for a blade optimized for AEP.

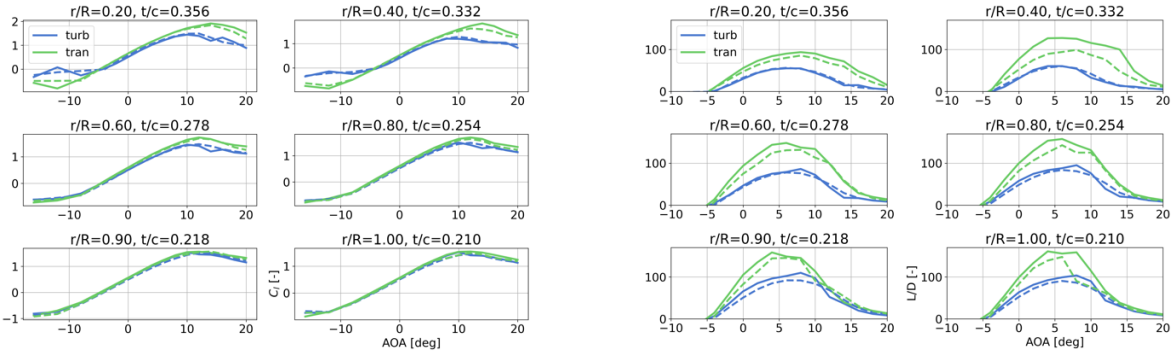

Figure 23: Performance of the airfoil series optimized for maximum rotor AEP. Left: Lift coefficient as funciton of angle of attack. Right: lift to drag ratio as function of angle of attack. Solid lines represent the surrogate predictions and dashed lines the 2D CFD evaluations.

Aerostructural design of the AMTB1 blade

The AMTB1 blade served as the baseline for comparison for designs with advanced tips, and needed to be fully optimized subject to constraints defined consistently across all the designs made in the project. The chosen turbine platform was the IEA 3.4 MW RWT developed in IEA Wind TCP Task 37, with an optimized rotor with a 16% larger rotor. The baseline turbine had a rotor diameter of 130 m, while the AMTB1 rotor had a diameter of 150 m resulting in a specific power of 192 Wm^{-2} vs 256 Wm^{-2}. This choice was made to match current marketed turbines across several OEMs. The blade was optimized based on the below defined optimization problem:

Objective: -AEP

Constraints

- max(torque) < 3.4.e6*1.06/max(rotor_speed)
- max(Steady state deflection) < 7.5 m

- max(Steady state gust deflection) < 12.5 m
- max(MxBR-steady-state) < 7256 kNm
- blade_mass < 16.2 ton
- blade_mass_moment < 3180 kNm
- max(strain_failure_index) < 1.0
- Ct_local < 0.9
- Various geometric constraints
- Frequency contraints:
    - Flapwise freqency constraint: (gamma_f * 3 * f_rot) / f_flap (gamma_f=1.1)
    - Edgewise freqency constraint: (gamma_f * 4 * f_rot) / f_edge (gamma_f=1.1)

Design variables:

- Planform: Bezier offset splines of chord, twist, relative thickness, pitch axis
- Bezier offset splines of SS and PS spar cap thicknesses
- Linear offset splines of leading and trailing edge (PS and SS) glass UD reinforcement thicknesses
- Tip speed ratio (constant below rated power)
- Blade pitch at all wind speeds

Two sets of steady-state aero-elastic computations were evaluated in the workflow, one for standard operating conditions and another considering a gust case, where the wind speed is computed as:

$$V_{gust} = V_0 + sU*g$$

where

$$sU = c * I_{ref} * (0.072 * (V_{ave}/c+3.0)*(V_0/c-4)+10)$$

$$V_{ref} = 37.5$$

$$V_{ave} = 0.2 * V_{ref}$$

$$c = 2.0$$

While a static solution cannot correctly predict design loads compared to time-domain simulations with inflow turbulence, a static gust case can help drive the design towards a load reducing geometry. The AMTB1 planform is shown in Figure 24, and its steady state response is shown in Figure 25.

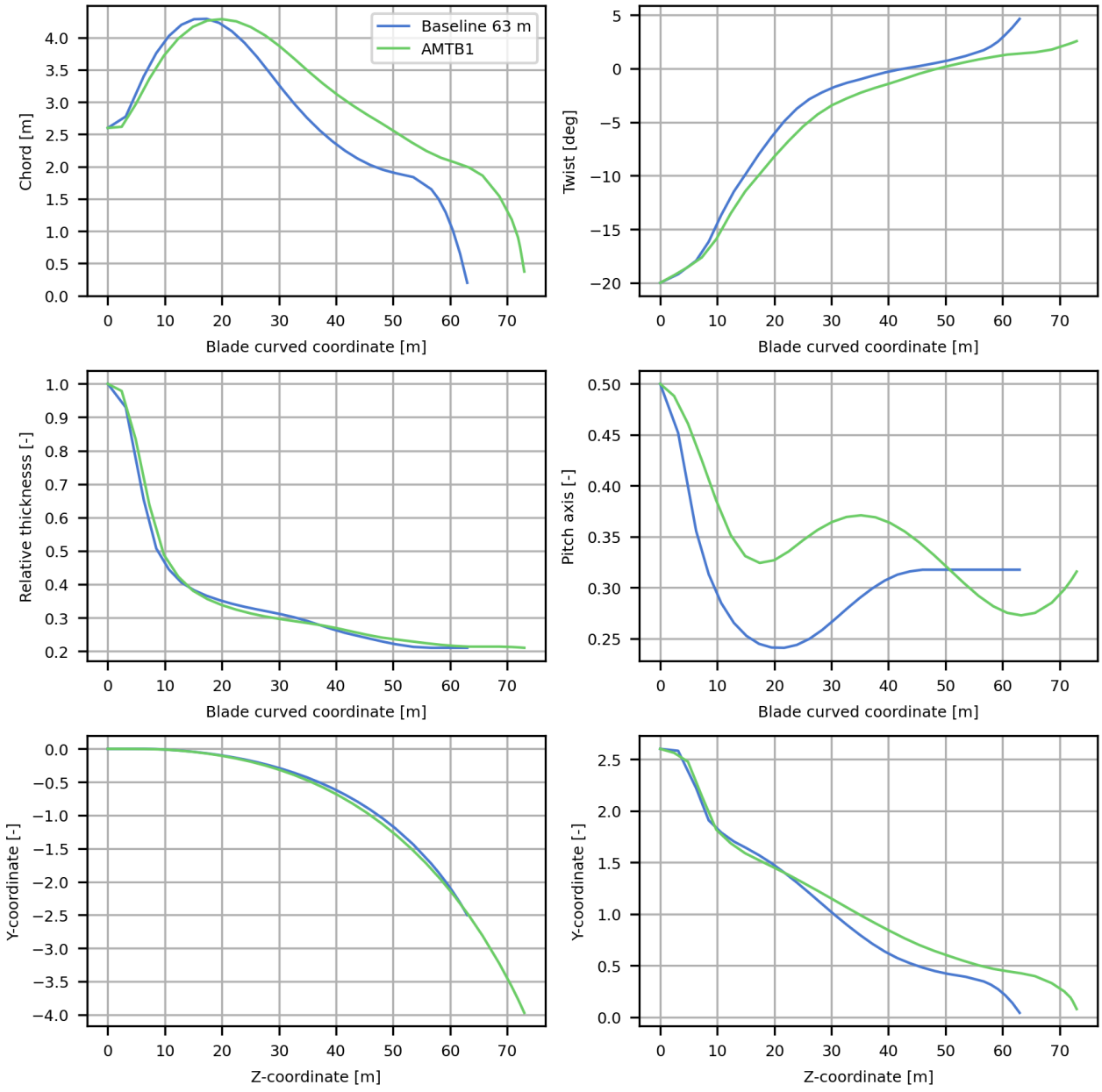

Figure 24: Planform of the AMTB1 blade

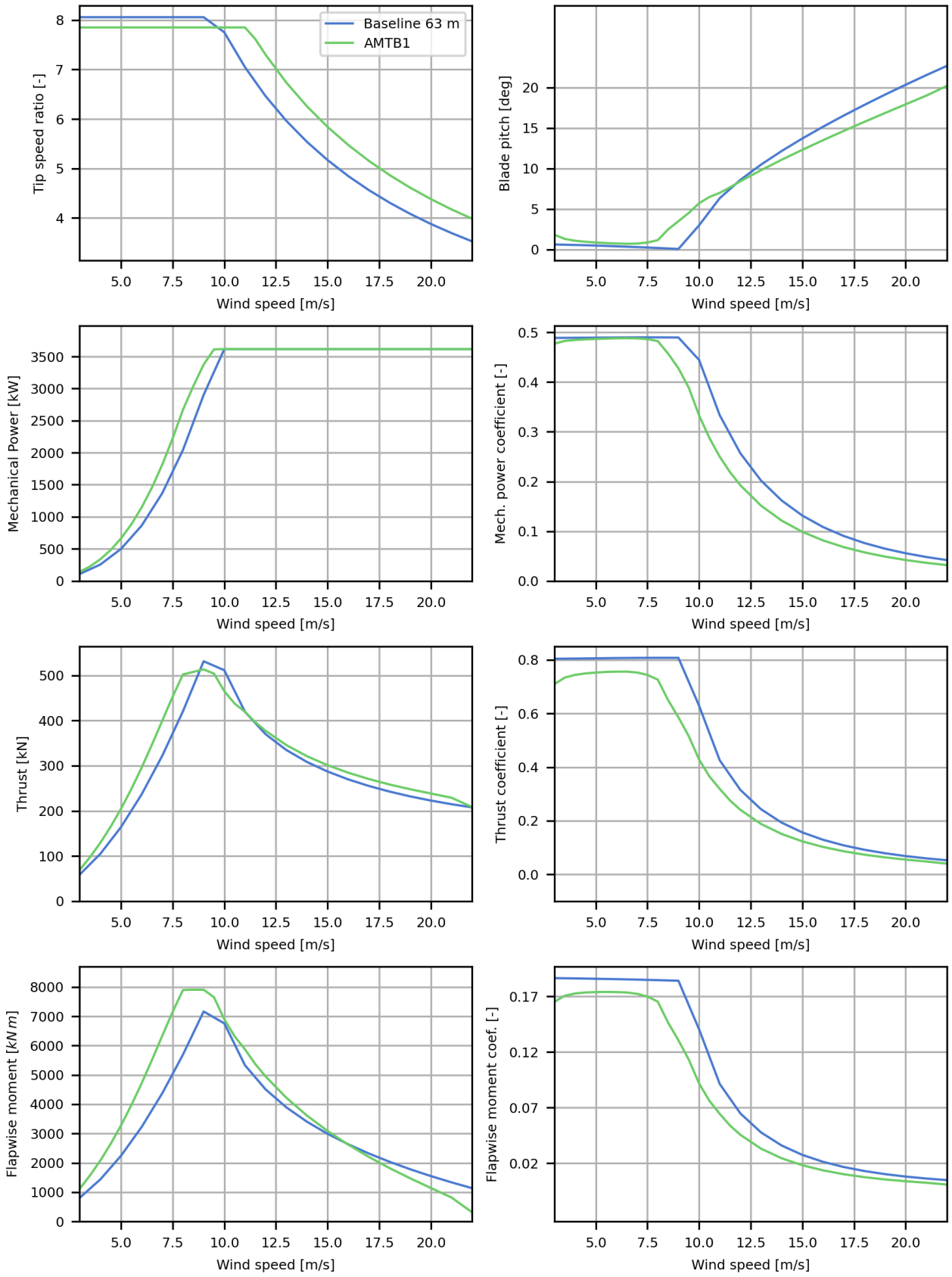

Figure 25: Steady state power curve and loads for the AMTB1 rotor.

Loads evaluation with HAWC2 (AMTB1)

The rotor design AMTB1 has been integrated in the HAWC2 model of the wind turbine platform of the IEA-3.4MW-RWT , where the controller settings have been tuned in HAWCStab2 and the blade structural damping parameters tuned in HAWC2. The model has been simulated in a reduced design load basis (DLB) setup (IEC class IIIA, k=2, shear a=0.2, DLC1.0 (clean steady-state), DLC1.2 (normal power production), DLC1.3 (extreme turbulence), yaw misalignment of +/- 8deg, 6 seeds per wind speed/direction bin) .

The comparison of power curves extracted from the time simulations with ideal (DLC 1.0) and operational (DLC 1.2) conditions is shown in Figure 26. The increase in AMTB1 AEP compared to baseline IEA-3.4-RWT is +4.25% (DLC1.0) and +3.17% (DLC1.2).

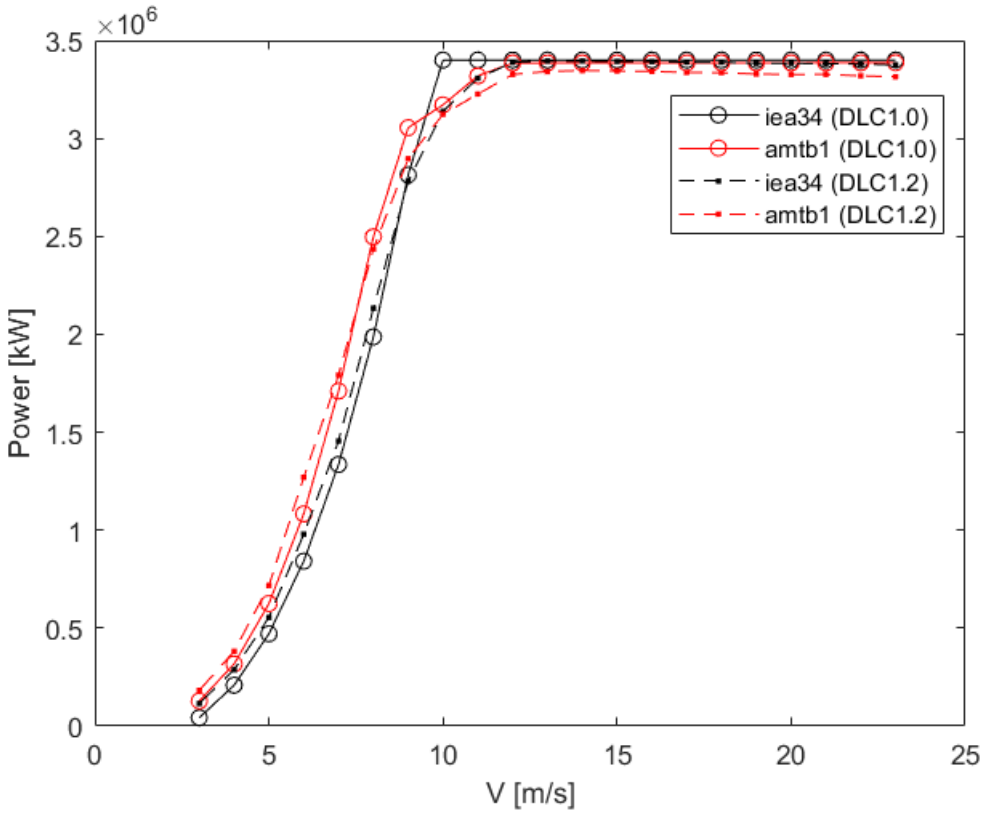

Figure 26: Power curve comparison between AMTB1 and IEA-3.4MW-RWT for ideal (DLC1.0) and operational (DLC1.2) conditions.

The lifetime ultimate and fatigue load envelopes of all turbine component interfaces of AMTB1 compared to the baseline IEA-3.4MW-RWT are shown in Figure 27-Figure 31. The spanwise distributions of the ultimate and fatigue load envelopes are shown in Figure 32.

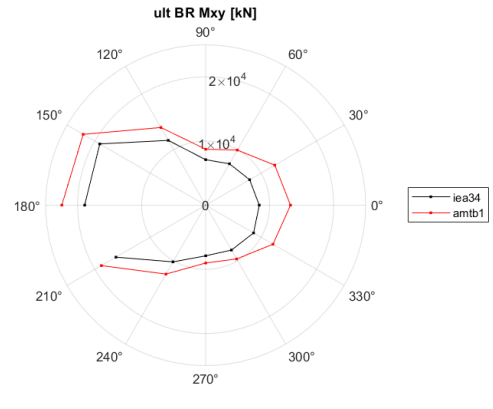

Ultimate.

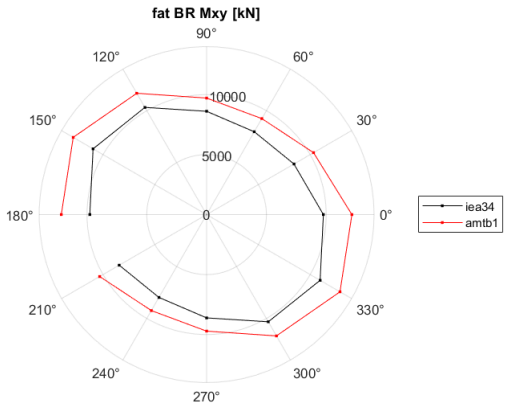

Fatigue.

Figure 27: Comparison of blade root load envelopes between AMTB1 vs IEA-3.4MW-RWT.

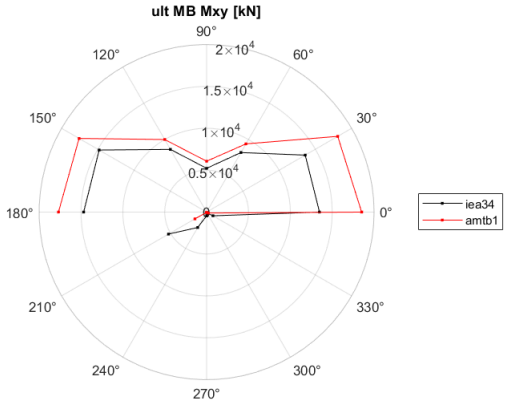

Ultimate.

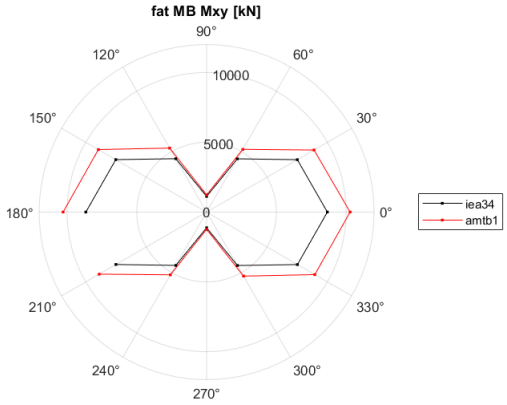

Fatigue.

Figure 28: Comparison of main bearing load envelopes between AMTB1 vs IEA-3.4MW-RWT.

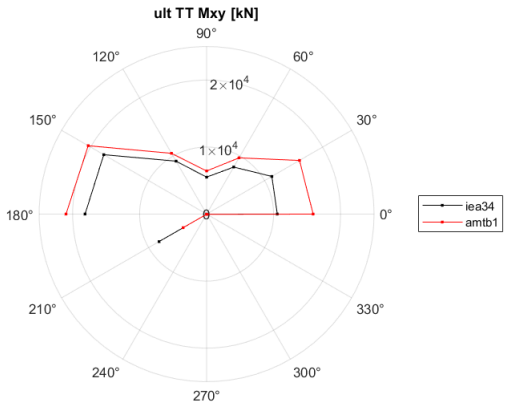

Ultimate.

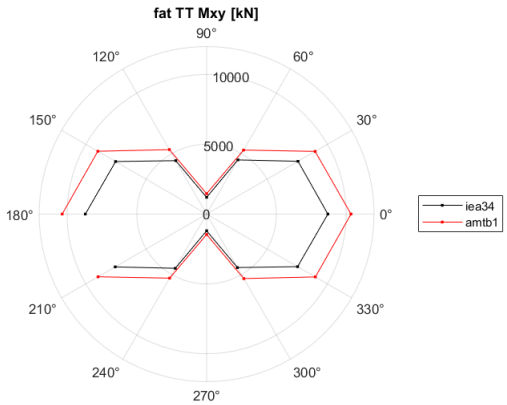

Fatigue.

Figure 29: Comparison of tower top load envelopes between AMTB1 vs IEA-3.4MW-RWT.

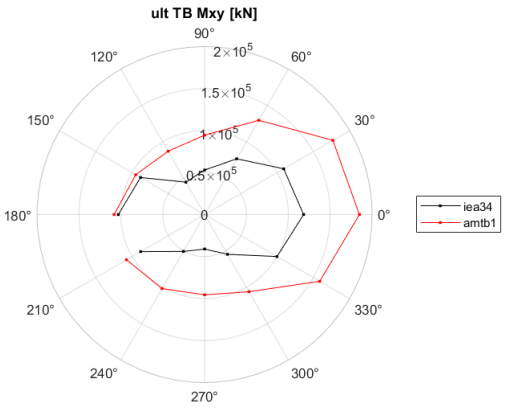

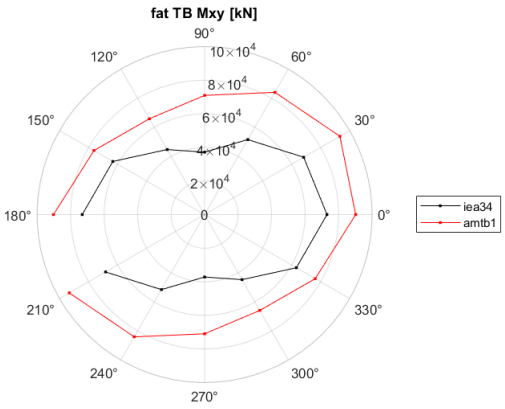

Ultimate. *Fatigue.*

Figure 30: Comparison of tower bottom load envelopes between AMTB1 vs IEA-3.4MW-RWT.

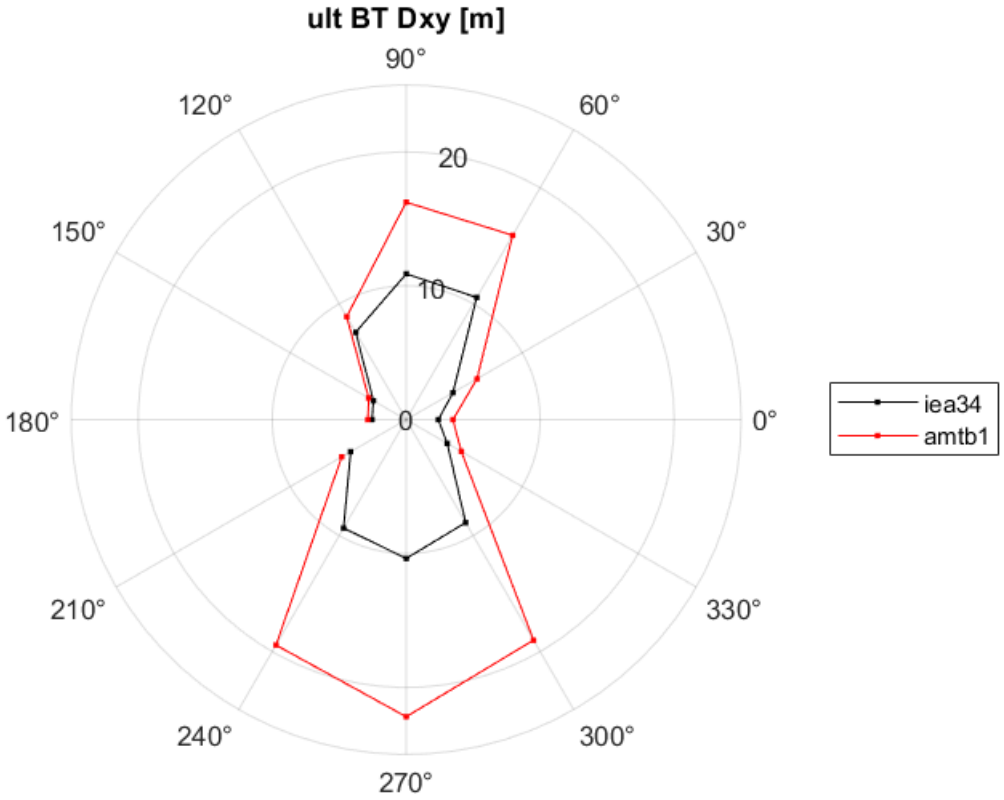

Figure 31: Comparison of blade tip deflection envelopes between AMTB1 vs IEA-3.4MW-RWT.

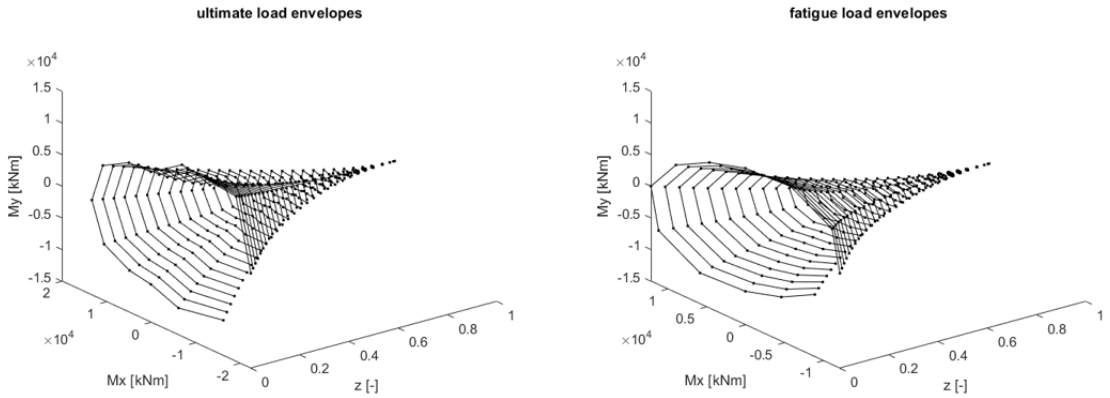

Ultimate. *Fatigue.*

Figure 32: Spanwise distribution of blade root load envelopes for AMTB1.

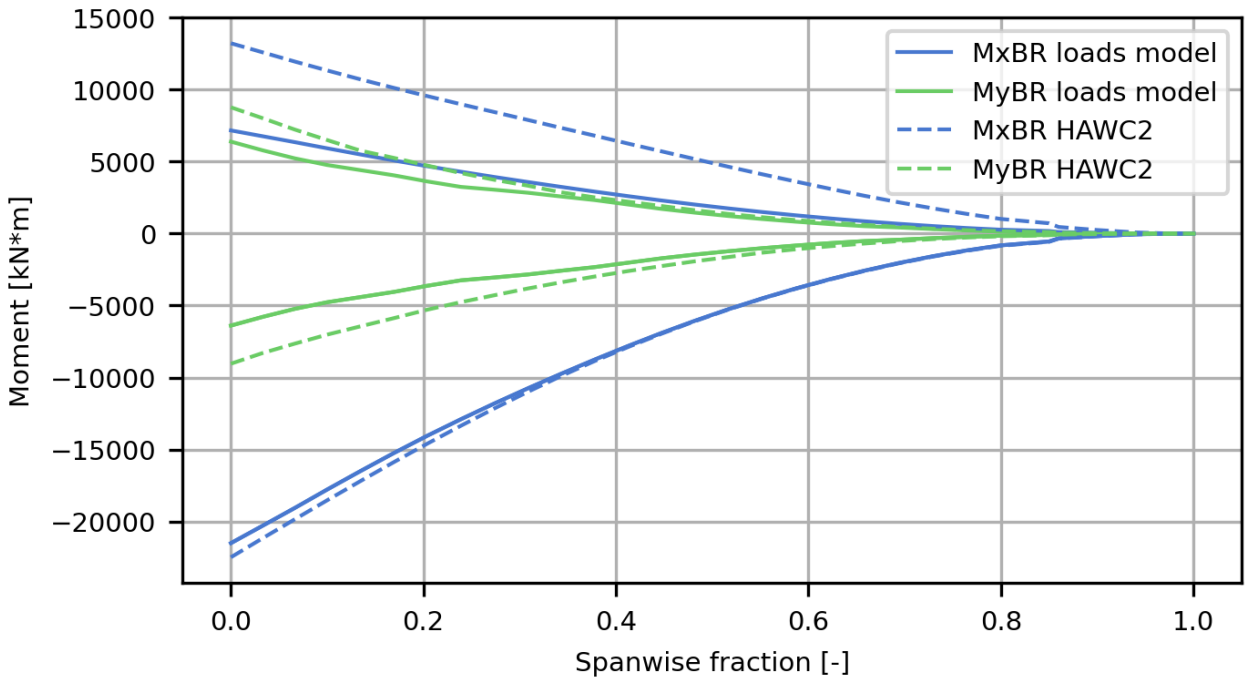

Figure 33: Comparison of extreme loads predicted with the analytical loads model used in AESOpt with loads predicted using HAWC2.

Figure 33**Fejl! Henvisningskilde ikke fundet.** shows a comparison of the extreme loads predicted by the analytical loads model used in AESOpt with time-domain loads from HAWC2. The comparison shows that the negative flapwise moment which sizes the spar cap is predicted well, while the positive flapwise moment is under-predicted. The edgewise loads are under-predicted by approximately 20%, which in particular could affect the edgewise reinforcement in the blade root.

Advanced tip aerodynamic exploration and validation using 3D CFD

To explore the aerodynamic design space more freely without structural constraints an aerodynamics-only design study was carried out with a fixed rotor diameter of 150 equivalent to the AMTB1 evaluated at 8 m/s only. Table 1 summarises the optimization setup for the three blades B3, B5, B9. All blades were optimized for maximum power with a constraint on steady-state flapwise moment equal to that of the AMTB1 blade, with design variables for chord and twist and optionally the outer 20% in-plane and out-of-plane tip shape in the case of B5 and B9. B3 served as a baseline and was a straight blade; B5 imposed no constraints on the tip shape, while B9 imposed both geometric and local loads constraints to suppress modelling features leading to unrealistic aerodynamic gains.

Table 1: Summary of the aerodynamics-only blade optimizations using BEVC.

Blade name	**Descriptions**
B3	B3: DVs: pf, Cons: loads, model: VC+NW
B5	B5: DVs: pf+tip_x/y, Cons: None, model: VC+NW
B9	B9: DVs: pf+tip_x, Cons: geometry, loads, Ct_local, model: VC+NW+flow-corr
B3_cfd	B3 - 3D CFD transition, n=7
B5_cfd	B5 - 3D CFD transition, n=7
B9_cfd	B9 - 3D CFD transition, n=7

Figure 34 and Figure 35 show the blade chord and twist and blade axis of the three blades. Without geometric constraints B5 finds a wavy tip shape, which can be attributed to the underlying vortex model in BEVC which predicts unrealistic gains from very high loading at the tip, combined with smaller gains from the wavy tip shape. In B9 constraints were imposed on the geometry of the tip as well as the local thrust coefficient which was found to be too high in B5.

To validate the predicted aerodynamic performance with the medium-fidelity code BEVC, 3D CFD blade resolved computations of the rotors were carried out using DTU's in-house CFD code EllipSys3D. Figure 36 and Figure 37 show a comparison of difference in local power and thrust coefficients relative to blade B3 for blades B5 and B9. Blue lines are predictions with BEVC while green lines are predictions with 3D CFD. There is a very good match between the two codes, although BEVC tends to overpredict the gain in power coefficient very close to the blade tip. On the contrary BEVC appears to under-predict the peak further inboard on the tip. B9 was optimized with geometric constraints to avoid a wavy shape and to avoid the locally very high loading found for blade B5, and therefore represents a significantly more realistic design. Table 2 summarises the results of the numerical optimizations and the evaluations using 3D CFD, and shows that

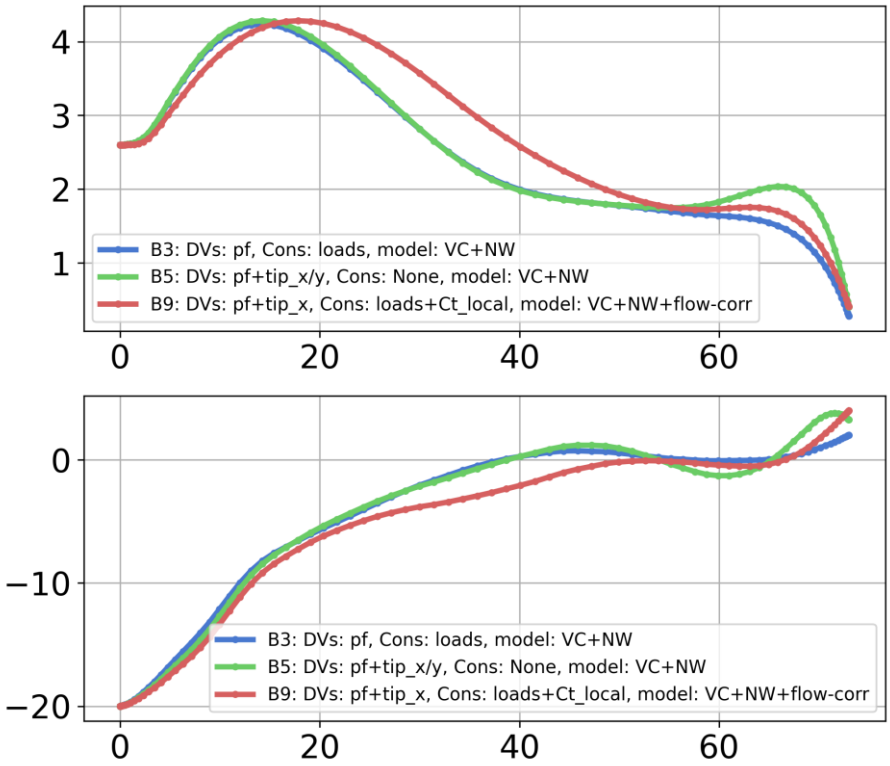

Figure 34: Blade chord and twist for the aerodynamically optimized blades B3, B5 and B9.

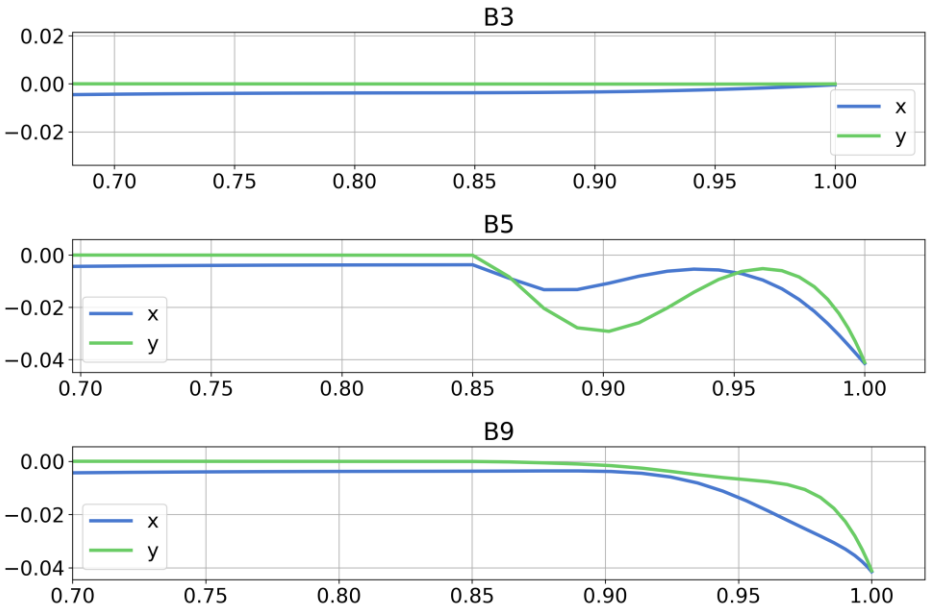

Figure 35: Blade axis in-plane (x) and out-of-plane (y) coordinates close to the tip. Notice that B3 has no prebend, which was not needed in this aerodynamics-only study.

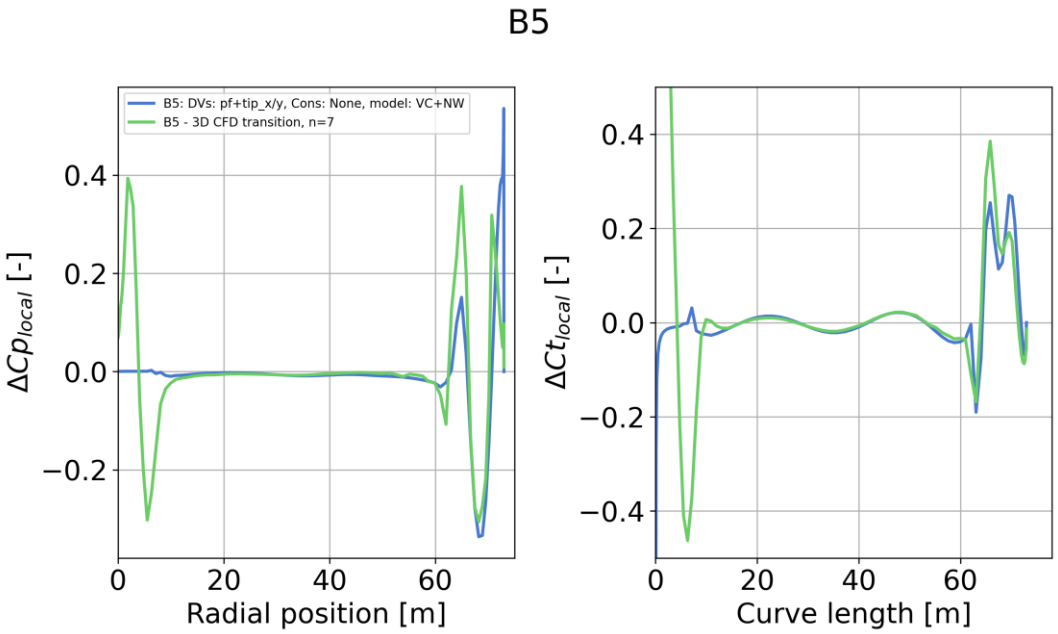

Figure 36: Comparison of change in local power and thrust coefficients of blade B5 relative to B3 with results of BEVC using the NW+VC model in blue and 3D CFD in green.

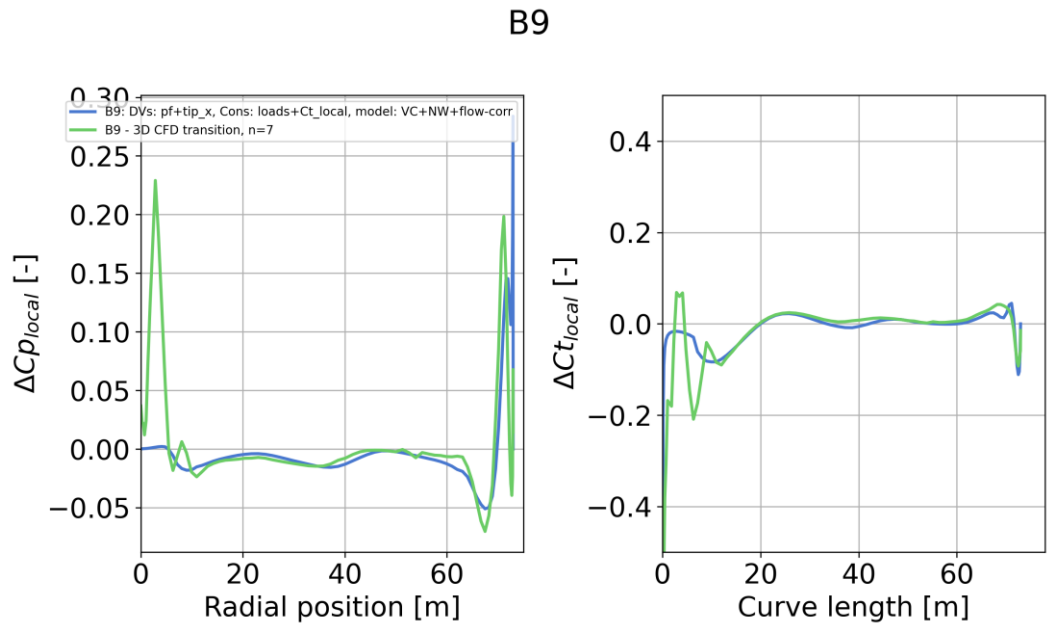

Figure 37: Comparison of change in local power and thrust coefficients of blade B9 relative to B3 with results of BEVC using the NW+VC model in blue and 3D CFD in green.

Table 2: Summary of results of the three blade optimizations and comparison to 3D CFD results.

Quantity	B3	B5	B9	B3_cfd	B5_cfd	B9_cfd
Power coefficient [-]	0.513 (0.000%)	0.559 (8.822%)	0.537 (4.531%)	0.534 (0.000%)	0.546 (2.243%)	0.544 (1.904%)
Thrust coefficient [-]	0.843 (-39.081%)	0.908 (-33.707%)	0.860 (-36.321%)	0.858 (-37.795%)	0.918 (-36.399%)	0.880 (-36.611%)
Power [kW]	2845.552 (0.000%)	3096.598 (8.822%)	2974.496 (4.531%)	2957.961 (0.000%)	3024.310 (2.243%)	3014.266 (1.904%)
Thrust [kN]	583.882 (0.000%)	629.009 (7.729%)	595.495 (1.989%)	594.396 (0.000%)	635.956 (6.992%)	609.675 (2.571%)

Aerostructural design of the AMTB2 blade with a curved tip

Based on the findings in the aero-only optimizations of blade tips and validations using high-fidelity 3D CFD evaluations, a blade was optimized allowing an advanced tip shape with both dihedral and sweep, modelled with the BEVC NW-VC model to capture the aerodynamic effects of the out-of-plane tip. The blade was designed to not exceed the loads of the AMTB1 blade and also maintained the same blade mass solving an optimization problem with the same objective and constraints but with additional design variables for the tip geometry. The blade structure was altered such that the outer 85% of the blade was a separate layup from the inner part of the blade, essentially treating it as a modular blade using separate molds for the two blade parts. This blade was named AMTB2.

The AMTB2 blade was found to increase the power production below rated with approximately 7% compared to the baseline AMTB1 blade (see Figure 40), which in turn had an efficiency gain of approximately 30% below rated compared to the IEA 3.4 MW RWT. In terms of AEP, AMTB2 had an increase of 2.1% compared to AMTB1, which is significant, given that it is load neutral, see Figure 41 that compares the extreme loads predicted for AMTB1 and AMTB2 by the analytical loads model implemented in AESOpt. Further high-fidelity modelling of the AMTB2 blade is, however, needed to verify the achieved gains, since it was observed that the medium-fidelity model had a tendency to over-predict the aerodynamic gains from curved tips.

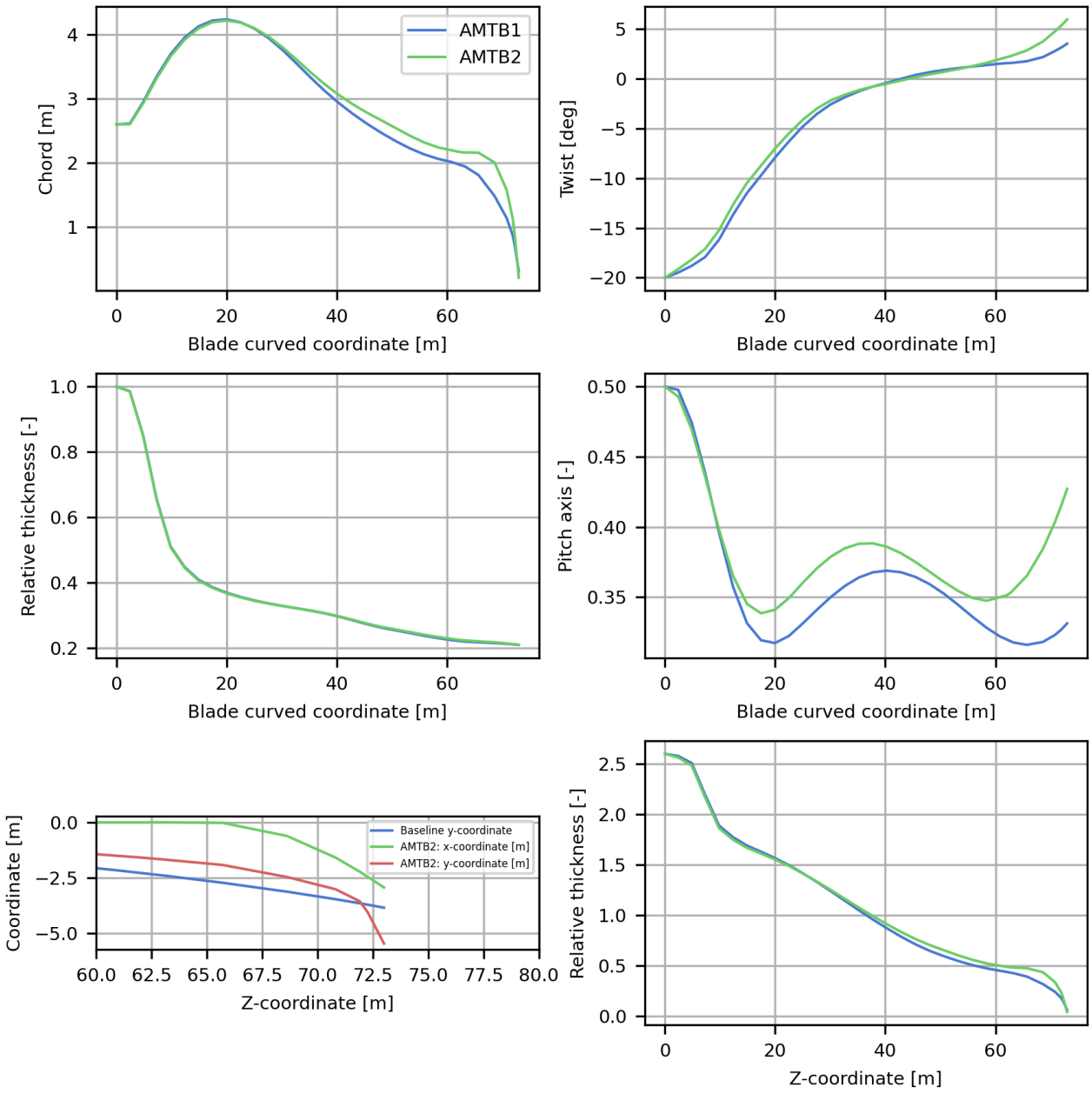

Figure 38: Blade planform of the AMTB2 blade.

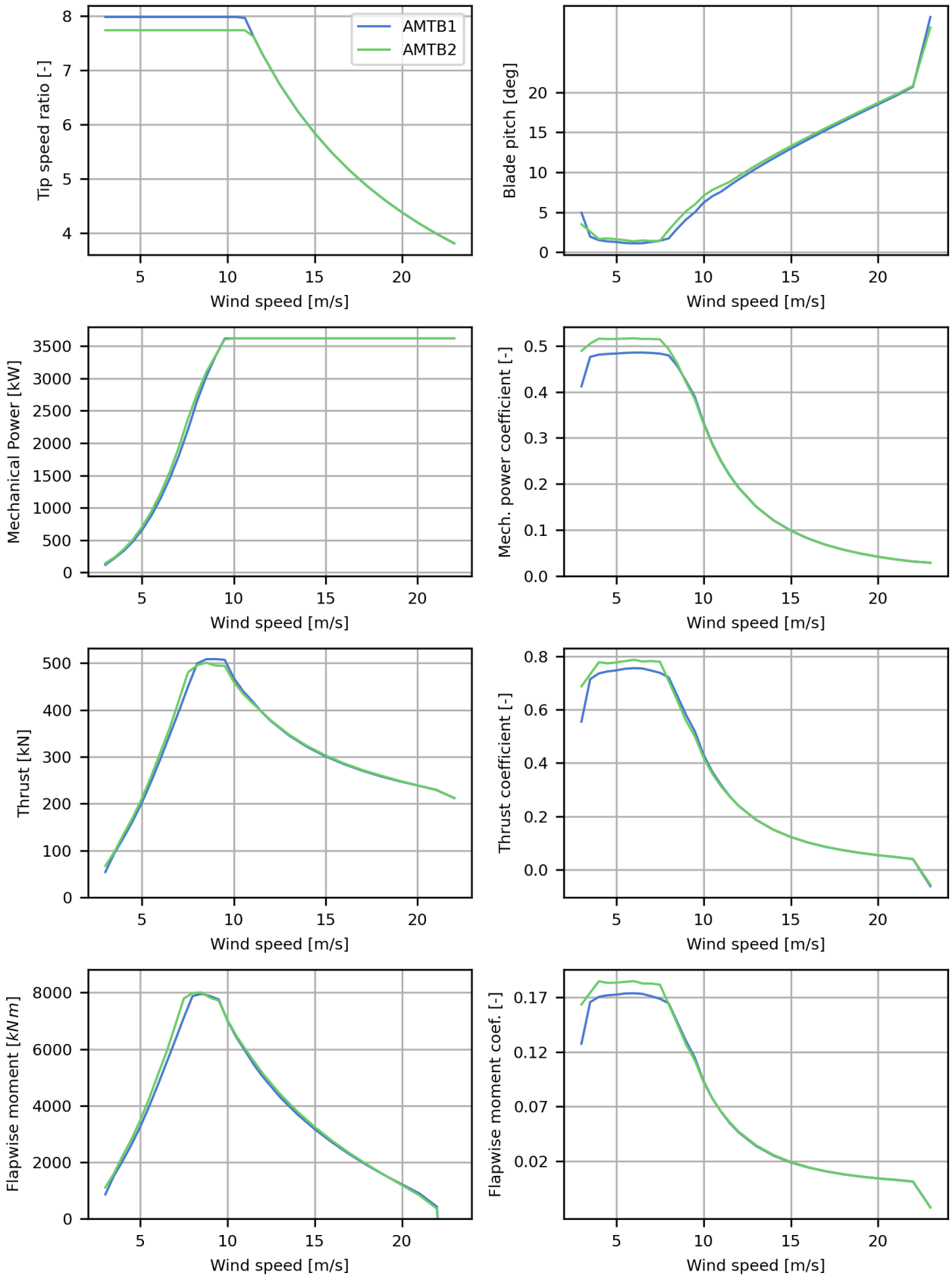

Figure 39: Steady-state power curve and loads for the AMTB2 rotor

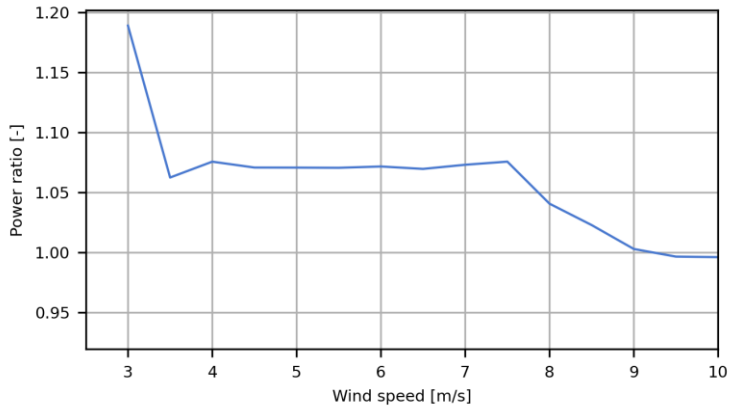

Figure 40: Ratio of mechanical power production below rated for AMTB2 vs AMTB1 showing an approximately 7% increase in power between 4-8 m/s.

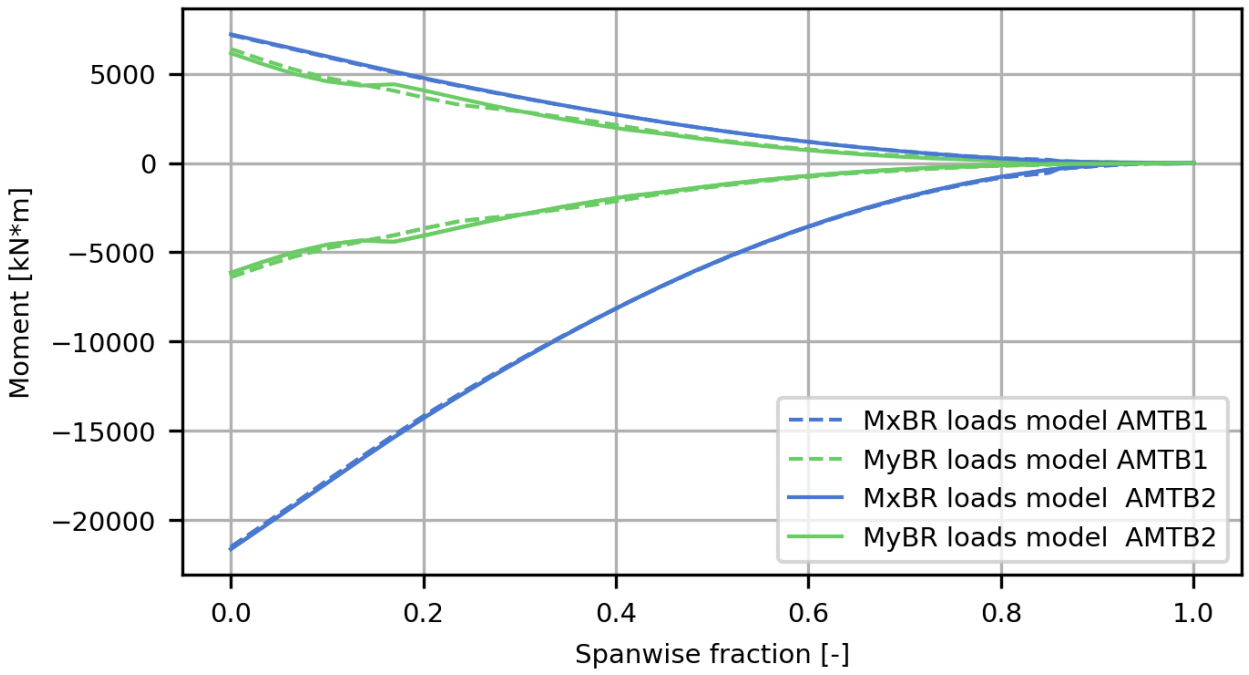

Figure 41: Comparison of extreme loads for blades AMTB1 and AMTB2 predicted with the analytical loads model used in AESOpt.

WP3: Laboratory scale experiments

The work package 3 aim was validation of the structural characteristics of aeroelastically tailored blades with advanced tip shapes. Initially it was composed of two phases: the first phase was focused on validation of cross-sectional tool used within a project and the second one on testing the 4m tip with high degree of sweep. Due to time constraints and lack of resources the second phase was cancelled. The first phase was converted

into comparison of structural response of a simple structure made of unidirectional laminate (tube) with material rail shear tests[4] performed on same material at LM Windpower.

It is well known that unidirectional laminates in shear will demonstrate high level nonlinearity, therefore obtaining shear modulus during postprocessing results becomes not so trivial task. ASTM standard[4] defines default shear modulus this way “Calculate the shear chord modulus of elasticity using Eq 6, applied over a 4000±200με engineering shear strain range, starting with the lower strain point in the range of 1500 to 2500με inclusive” (p.13). The standard also allows a user to come up with their own definition “Shear Modulus of Elasticity (Other Definitions) — Other definitions of elastic modulus may be evaluated and reported at the user’s discretion”. The difference of different shear modulus definitions can be demonstrated using curves from Montana University report[5] and processing presented in Figure 42.

Table 1. Average 3-D elastic and strength properties for thick unidirectional glass fabric/epoxy laminate and for neat resin.

LAMINATE ELASTIC CONSTANTS[1]	V_F = 56.8 – 58.2%
Tensile Modulus E_L (GPa)	44.6
Tensile Modulus E_T (GPa)	17.0
Tensile Modulus E_Z (GPa)	16.7
Compressive Modulus E_L (GPa)	42.8
Compressive Modulus E_T (GPa)	16.0
Compressive Modulus E_Z (GPa)	14.2
Poisson Ratio ν_{LT}	0.262
Poisson Ratio ν_{LZ}	0.264
Poisson Ratio ν_{TL}	0.079
Poisson Ratio ν_{TZ}	0.350
Poisson Ratio ν_{ZL}	0.090
Poisson Ratio ν_{ZT}	0.353
Shear Modulus G_{LT} (GPa)	3.49
Shear Modulus G_{LZ} (GPa)	3.77
Shear Modulus G_{TL} (GPa)	3.04
Shear Modulus G_{TZ} (GPa)	3.46
Shear Modulus G_{ZL} (GPa)	3.22
Shear Modulus G_{ZT} (GPa)	3.50

[1]Tensile and compressive moduli and Poisson's ratios determined from best fit line between 0.1% and 0.3% strain; shear moduli calculated from best fit line between 0.2% and 0.6% shear strain.

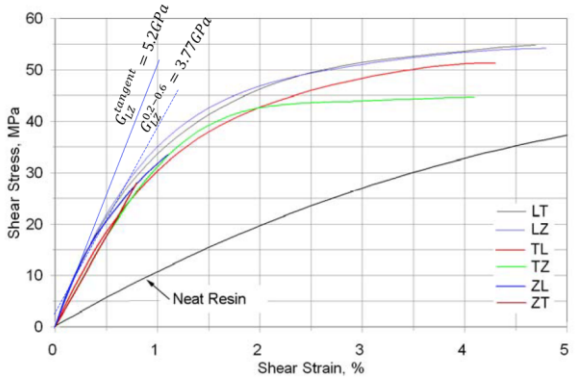

Figure 42: Shear modulus processing with different methods.

This report used chord modulus in the 2000-6000με range (which is a bit higher than standard recommends) and arrived to 3.77 GPa value. Other part of the spectrum will be tangential modulus which for this particular case will be 5.2 GPa. The difference between the two values is 38%. Which extreme case but in reality 20-30% difference can be expected if shear modulus defined based on standard procedure vs for the shear strain levels wind turbine blades usually exposed to. Due to reasonably thick caps in a glass wind turbine blade this difference can contribute into overall uncertainty of blade torsional response.

The purpose of rescoped test campaign was to show the effect of such postprocessing of material properties on torsional response and demonstrate it in a structural test.

For this purpose, set of moulds for casting a tube of 6 m long with 200 mm outer diameter was designed and manufactured (see Figure 43). The peculiarities of these moulds are that infusion done using so-called “one shot” technology when casted component manufactured with one infusion without adhesive joints. This approach allows to exclude uncertainty of adhesive properties and joint geometry on strain/stress distribution.

[4] ASTM D7078/D7078M-05 Standard Test Method for Shear Properties of Composite Materials by V-Notched Rail Shear Method 10.1520/D7078_D7078M-05

[5] www.montana.edu/composites/documents/3D%20Static%20Property%20Report.pdf (retrieved 25.02.2025)

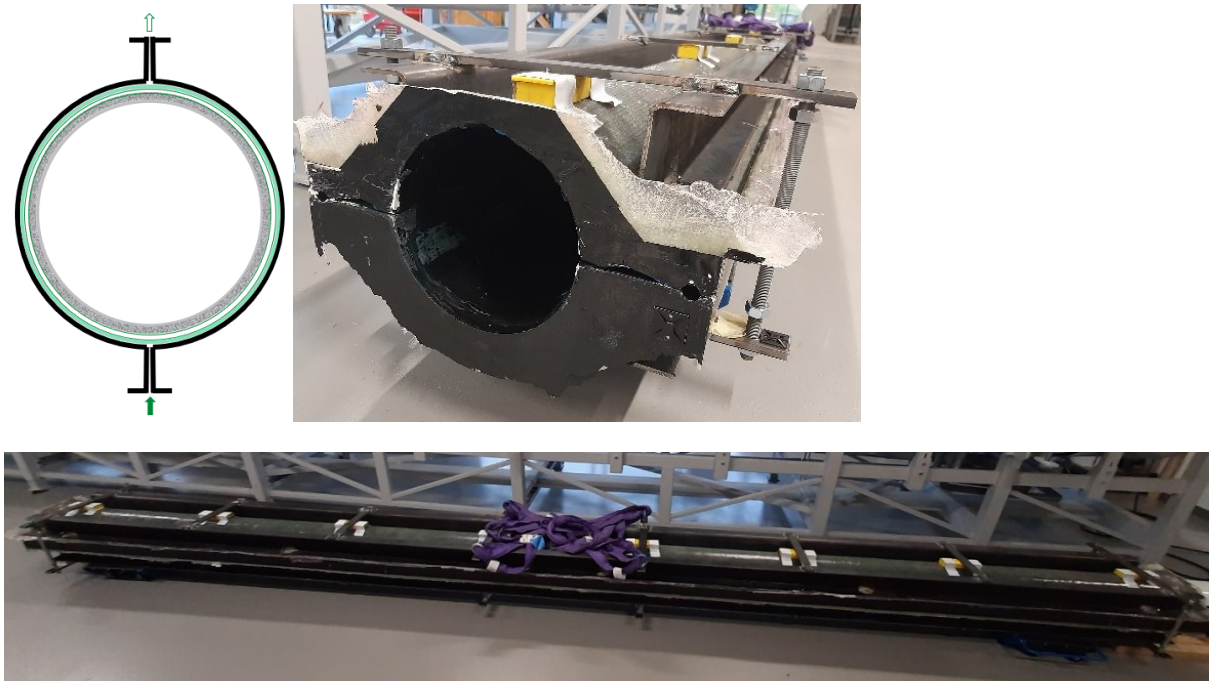

Figure 43: Moulds for tubes manufacturing.

Using this moulds series of tubes was manufactured (see Figure 44). One of them out of unidirectional fabric LM uses in their blades and rail shear coupons were made of.

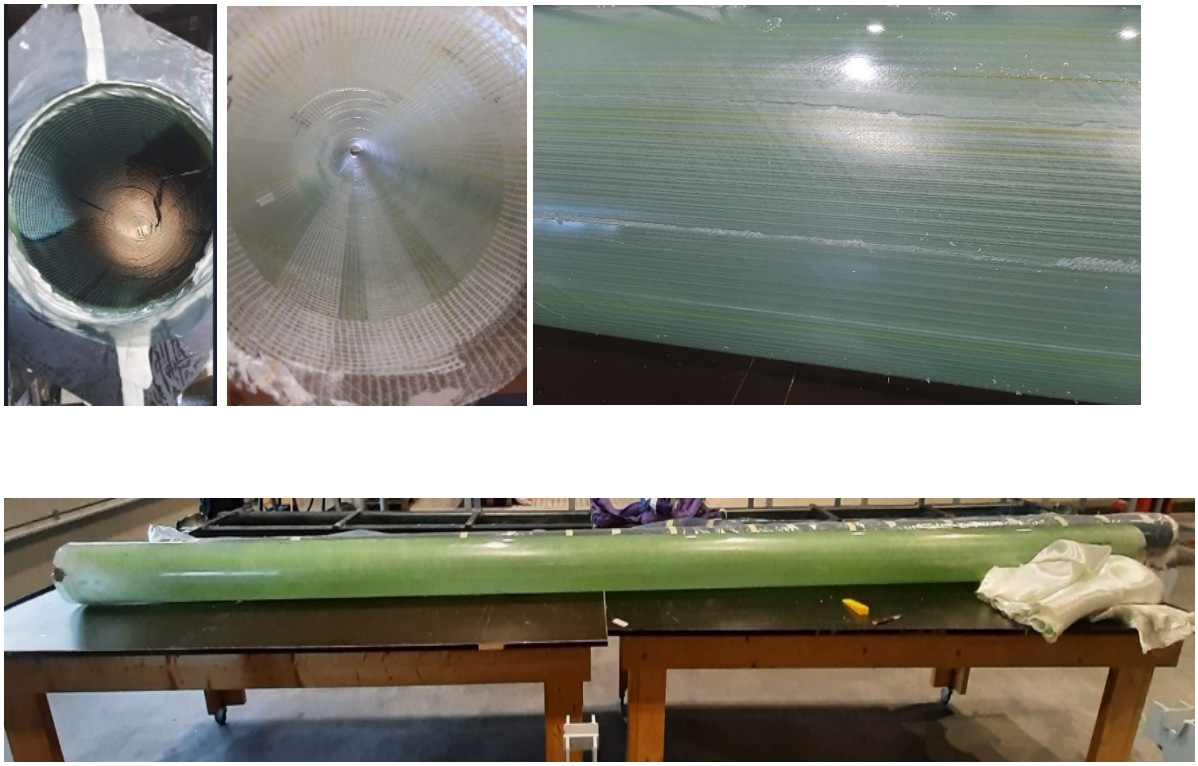

Figure 44: Infusion and casted tubes.

For tube loading in pure torsion a setup consisting of root clamp and tip clamp was designed and manufactured (see Figure 45). The torque is applied as pair of forces which are measured by two load cells and equalized in order to avoid applying shear load to the tube. The test campaign was not completed within the project duration and is still ongoing with the plan to be accomplished end of December 2025.

Figure 45: Test setup for applying pure torsion.

WP4: Detailed design (LM)

This section describes how LM has evaluated AMTB1. The idea was to construct a LM realistic (close to factory ready) structure based on DTU's HAWC2 loads and then compare blade properties and steady state behaviour between the DTU and the LM design.

Geometry

The AMTB1 planform parameters and seed airfoils were used as input to generate a 3D geometry in LM format. Therefore, there could be small deviations between the DTU and the LM geometry of AMTB1 due to deviations in DTU's and LM's lofting method.

Loads

The hawc2 extreme loads from DTU were converted to LM format.

Furthermore, the hawc2 timeseries from DTU were processed and used to generate the needed Markov matrices for including fatigue loads in the optimization and evaluation of a LM structure.

LM materials

To be close to reality we have used LM materials for the blade composite structure. Of course, we have chosen materials with similar properties (but not identical) as the glass-epoxy materials used in the DTU structure.

DTU vs LM design

As expected, we see some deviations between the two designs.

The most obvious difference is the fact that the LM design has included added masses in terms of lightning system, bushings, glue etc. which is not considered in the DTU design. That leads to differences in mass and static moment in the order of 10%.

Another obvious difference is that fatigue loads are accounted for in the LM design whereas this is not considered in the DTU design. Again, this leads to differences in mass and static moment in around 10%.

When added masses and fatigue loading is neglected in the LM design the mass properties are approaching and edge and flap stiffness lie within ±10 %. The deviations can be explained by the fact that the DTU design were optimized based on the simple load model whereas the HAWC2 loads were used in the LM design. Furthermore, the 3D geometry and the different materials could also play a role. Torsional stiffness is somewhat larger in the LM design and that could partly come from some manufacturing needed materials included in the LM design and some modelling differences. Mass, elastic and shear centers are pretty good aligned.

Again, when neglecting added masses and fatigue loading in the LM design and when using same pitch schedule some deviations are seen in the steady state behaviour of the DTU and the LM design. This is mostly due to the torsional stiffness, and this can be compensated by modifying the pitch schedule.

Conclusion and recommendation

Based on above observations it's clear that especially two factors, added masses and fatigue loading, play a major role for the deviations between the DTU and the LM structural design. Therefore, to enable LM to use the AESOpt tool for practical design work, these features need to be implemented.

Furthermore, the simple load model used in the DTU design also play a role for the deviations. However, the new loads surrogate model looks promising and that is yet to be tested and explored.

The remaining differences are due to different inputs, so that is not related to the AESOpt tool itself.

Curved and swept blade tips

The concept of having a curved and swept blade tip is from a manufacturing perspective of course more complicated than producing a straight one and therefore more costly. Consequently, for LM to adopt this technology in future blades, the potential AEP gains at equivalent load levels must outweigh the additional cost of the technology.

First, it is of course important to carry out further high-fidelity modelling to investigate if the 2.1 % AEP gain of AMTB2 is realistic. Additionally, extending the design space exploration may reveal even greater gains, which makes it a worthwhile direction for future work. Finally, determining whether the energy gain is sufficient to justify this new technology requires further investigation, which we look forward to seeing pursued in the future.

WP5: Prototype development and testing (LM)

Design and aerodynamic wind tunnel testing of airfoils for advanced blade tips

In parallel with tool developments and blade design work performed by DTU, LM has designed and validated a new airfoil family to be used for future advanced blade tip designs.

Acoustic performance of onshore wind turbines is often a design driver or a limiting factor for turbine operation, especially in Europe. Therefore, main requirements for the new airfoils focused acoustic performance.

The airfoils were design using existing LM design and optimization tools. These tools and methods are continuously being improved and validated. Specifically important for this work, are the acoustic predictions. During design phase, acoustic predictions were carried out using the LM in-house tool ADT2 (Acoustic Design Tool version 2). Both airfoil level and blade level acoustic performance can be assessed, and predictions have recently been improved and validated both by wind tunnel data on airfoils and by field measurements on full scale turbines. Besides acoustic performance also aerodynamic and structural performance of blades utilizing these low noise airfoils were used as performance metrics.

Four new airfoils were down selected to form a Low-Noise Airfoil Family consisting relative thicknesses of 15%, 18%, 21%, and 24%. In general, thinner airfoils give better acoustic performance, whereas thicker airfoils result in better structural performance, so a compromise is needed in the blade design. The 15% airfoil gave very little acoustic advantage over the 18% airfoil, so this was not considered for further validation. In a separate LM funded project, the other three airfoils were then tested in the Virgina Tech acoustic wind tunnel. The measured acoustic performance matched expectations quite well. Furthermore, the airfoils also performed quite well with noise reducing devices like serrations. Other characteristics like roughness sensitivity, which can be difficult to predict, showed good behaviour.

Since expected acoustic performance was achieved, these three airfoils were taken to the next validation step, which in this case was the aerodynamic wind tunnel testing. As part of the AMTip project, three airfoils were tested in the in-house LM wind tunnel, which can reach Reynolds numbers up to 6 million. Since LM wind tunnel has different size than the Virginia Tech wind tunnel, three new airfoil models were constructed for the testing. A total of 258 tests were performed to provide polars for range of Reynolds numbers, and with various add-ons like serrations. The measurements have been further processed and polars added to an internal LM database, so now airfoils are released to be used for new blade designs.

Based on LM database benchmark, the new Low-Noise airfoil family are characterized in:

- Best in class noise performance, including high wind speed noise
- Good for roughness sensitivity
- Average aerodynamic performance
- Average to low structural metrics

An existing LM blade was re-designed with the new low-noise airfoils. Compared to the baseline blade, a small loss in AEP (0.24%) was a good compromise to get lowest Levelized Cost of Energy (LCOE). Bonus of the lower loads airfoils is lower blade mass and material cost. The 1 dB(A) noise reduction target was achieved based on ADT2 predictions corrected with wind tunnel data. Overall, an LCOE reduction of 1.7% was calculated.

Conclusions and recommendations:

- A new Low-Noise airfoil family consisting of three airfoils have been designed and successfully validated by LM and is now released to be used for future blade designs.
- Overall, LM prediction methods (combining XFOIL and CFD) are predicting the aerodynamic polars quite well. Maximum lift seems consistently underestimated, so there is still need for improvements.
- Noise predictions are quite good in clean case, but miss tripped performance due to not correctly predicting flow separation and not accounting for physical impact of for example zigzag tape used in wind tunnels.
- Rotor noise reduction is now 1 dB(A) instead of previously 1.5 dB(A).

6. Utilisation of project results

The AMTip project developed the following technologies:

- **(DTU) General purpose multidisciplinary blade design framework AESOpt**, that consisted of state-of-the-art models developed by DTU, capable of modelling and optimizing blades with curved blade tips using the medium-fidelity aerodynamics code BEVC.
- **(DTU) Two conceptual blade designs AMTB1 and AMTB2** that numerically demonstrated the capabilities of the AESOpt design framework, in particular that a blade with an advanced blade tip could produce up to 2% increase in AEP compared to a standard blade tip.
- **(LM) State-of-the-art aero-acoustically optimized aerofoils** optimized for advanced blade tips with high aerodynamic performance, structural efficiency and low noise. One of these aerofoils was tested and validated in LM's own wind tunnel as part of the project.

Utilisation of the technological results

DTU will continue development of the AESOpt framework enabling research in blade and wind turbine design. The framework itself will become open source once sufficiently matured, allowing it to be used both for research purposes and for commercial use. AESOpt was made operational on LM Windpower computing systems, and LM project members were trained in the use of the framework through a series of workshops. The conceptual blade designs AMTB1 and AMTB2 serve as demonstrators for the possibilities with advanced curved blade tips, which LM used for internal design development and evaluations, although no specific products are under development features these specific designs. The LM-developed aerofoils were tested under relevant but controlled flow conditions in a wind tunnel and can be used commercially after project completion.

Utilisation of the commercial results

Advanced aerofoils is an essential technology for maintaining competitiveness in today's market. While the aero-acoustically optimized aerofoils developed by LM were not used in a commercial product developed within the project period, they have within the project been tested and validated to a level where they can be used in future products.

Competitive situation in the market

Globally, all wind turbine OEMs move towards rotors with larger swept area, while at the same time attempting to reduce blade mass and loads on the turbine platform. Blades with load neutral advanced tips have clear aerodynamic advantages but also impose added cost and complexity in manufacturing. The marked is characterised by increasing costs associated with wind turbine manufacturing, and increased focus on lowering CAPEX, making it challenging for OEMs to increase profit margins. These factors makes it more challenging to introduce new technology to the market.

Project contribution to energy policy objectives

The results of this project supports EUDP's strategy to mature renewable energy solutions and reduce wind energy costs. It has developed blade design innovations that could increase AEP of an onshore wind turbine by approximately 2% and the technology could also be applied to offshore turbines. The project established a strong collaboration between Danish research and industry, reinforcing Denmark's leadership in wind energy. Furthermore, the project aligned with the Megavind Annual Agenda 2020, aiming to advance blade design through modeling, validation, and testing.

7. Project conclusion and perspective

The overall objective of the AMTip project was to develop wind turbine blade design solutions featuring advanced curved tips made possible from advanced manufacturing techniques such as additive manufacturing. To enable such blade designs, a complex software framework using DTU's research-based tools was successfully implemented featuring the aerodynamic code BEVC that enabled prediction of aerodynamic loads on blades with curved tips at a computational cost comparable to standard Blade Element Momentum codes used in industry. The framework was applied to design a series of conceptual blade designs exploring the complex aero-elastic design space of the combined aerodynamic and structural design variables. The results showed that blades with advanced blade tips could gain up to 1-2% in annual energy production (AEP) without increasing loads compared to a blade designed with a conventional blade tip. The blade designs were subsequently evaluated by LM and internal design investigations were carried out aligning the designs with LM design practices. Additionally, LM developed two new aerofoils dedicated to advanced blade tips balancing aerodynamic performance, low noise and structural efficiency. These aerofoils were experimentally validated in LM's own wind tunnel.

To mature the developed blade technologies, further detailed design and validation is needed, in particular the detailed structural design using advanced manufacturing techniques enabling highly curved blade tips, which was not addressed in the present project.

8. Appendices

Publications related to and partially or fully funded by the project:

- Zahle, F., Li, A., Lønbæk, K., Sørensen, N. N., & Riva, R. (2024). Multi-fidelity, steady-state aeroelastic modelling of a 22-megawatt wind turbine. In *The Science of Making Torque from Wind (TORQUE 2024):* Article 022065 IOP Publishing. https://doi.org/10.1088/1742-6596/2767/2/022065 (core development of method financed by AMTip, application to a 22 MW turbine financed in another project)
- Gaunaa, M., Sørensen, N. N., & Li, A. (2024). A correction model for the effect of spanwise flow on the viscous force contribution in BEM and Lifting Line methods. In *The Science of Making Torque from Wind (TORQUE 2024):* Article 022068 IOP Publishing. https://doi.org/10.1088/1742-6596/2767/2/022068
- Barlas, T., Göçmen, T., & Riva, R. (2024). Development of a machine learning model for wind turbine fatigue and ultimate loads based on static loads. In *The Science of Making Torque from Wind (TORQUE 2024):* Article 052009 IOP Publishing. https://doi.org/10.1088/1742-6596/2767/5/052009
- S Dicholkar, A., Lønbæk, K., Zahle, F., & Sørensen, N. N. (2024). Stabilization of SIMPLE-like RANS solvers for computing accurate gradients using the complex-step derivative method. In *The Science of Making Torque from Wind (TORQUE 2024):* Article 052022 IOP Publishing. https://doi.org/10.1088/1742-6596/2767/5/052022
- Li, A., Gaunaa, M., Pirrung, G. R., & Lønbæk, K. (2024). How does the blade element momentum method see swept or prebent blades? In *The Science of Making Torque from Wind (TORQUE 2024):* Article 022033 IOP Publishing. https://doi.org/10.1088/1742-6596/2767/2/022033
- Dicholkar, A., Lønbæk, K., Madsen, M. H. A., Zahle, F., & Sørensen, N. N. (2025). From bluff bodies to optimal airfoils: Numerically stabilized RANS solvers for reliable shape optimization. *Aerospace Science and Technology*, *161*, Article 110153. https://doi.org/10.1016/j.ast.2025.110153